Economic Geology
Vol. 90, 1995, pp. 17–36

Carlin Gold Deposits, Nevada: Origin in a Deep Zone of Mixing between Normally Pressured and Overpressured Fluids

CARL A. KUEHN

IMDEX INC., P.O. Box 65538, Tucson, Arizona 85717

AND ARTHUR W. ROSE

Department of Geosciences, Pennsylvania State University, University Park, Pennsylvania 16802

Abstract

Gold mineralization at Carlin is clearly younger than hydrocarbon maturation (pre-Cretaceous) and felsic dike intrusion (Cretaceous), and older than deep oxidation (late Tertiary). Within the episode of gold mineralization, the main gold ore (MGO) stage and late gold ore (LGO) stage are distinguished paragenetically, with a variety of vein and mineralization types in each. MGO stage fluids contained 5 to 10 mole percent CO_2, appreciable H_2S, and 3 ± 1 wt percent NaCl equiv. At least portions of MGO stage mineralization were characterized by two-phase boiling (CO_2 exsolution) at 215° ± 30°C and 800 ± 400 bars. In contrast, LGO stage fluids were gas poor with salinities ≤1.5 wt percent NaCl equiv and record only nonboiling conditions. MGO stage fluids had $\delta^{18}O_{H_2O}$ values of 5 to 9 per mil, whereas LGO stage fluids resembled unevolved meteoric water with $\delta^{18}O_{H_2O}$ values ≤ −3 per mil.

From the MGO stage to the LGO stage, calcite $\delta^{18}O$ values shifted from near whole-rock values of 12 ± 3 per mil to around 0 ± 1 per mil as LGO stage fluids flooded the system. Jasperoids also record a large range (9–22‰) in $\delta^{18}O_{H_2O}$ values. These data indicate the involvement of two very different fluids in ore deposition. Because MGO and LGO stage features are closely associated spatially with each other and with Au, As, Sb, Hg, and other ore elements, both fluids are believed to have both been present during most stages of ore deposition.

At pressures of 80 to 85 percent lithostatic, depths of 3.8 ± 1.9 km are required to accommodate the 800 ± 400 bars of pressure recorded in MGO stage fluid inclusions. Carlin, therefore, is not an epithermal or hot spring deposit. Carbon dioxide in gas-rich MGO stage fluids may have originated either directly from buried intrusions or their contact aureoles, or from low-grade regional metamorphism at depth. The water may have been originally meteoric, and Au may be magmatic or derived from leaching of deep metamorphic or sedimentary rocks. Ore deposition appears to have occurred in zones of throttling at a pressure seal between normally pressured and overpressured regimes, where fluids experienced a change from near-lithostatic to hydrostatic conditions. Such pressure seals are common in deep sedimentary basins and may be a key to highly localized gold deposition. Mixing of two fluids and interaction with host rocks along thin permeable bioclastic horizons are believed to have been the major factors in depositing ore.

Introduction

THE Carlin sedimentary-hosted gold deposit, located in north-central Nevada and discovered in 1962, has produced about 150 tons of gold (Fig. 1). It is the type deposit of the most important group of gold mines developed in the United States since about 1940 and is one of the largest such deposits.

Geologic and geochemical similarities between Carlin and many other carbonate-hosted disseminated gold deposits in Nevada suggest that the same general set of processes has operated in various places to produce the many Carlin-type deposits (Bagby and Berger, 1985). Prior investigations at Carlin led to the concept that gold mineralization occurred in the shallow levels of a meteoric-water hydrothermal system driven by the heat of Miocene igneous activity in north-central Nevada (Radtke et al., 1980; Radtke, 1985; Rye, 1985). Recent radiometric dating indicates that gold mineralization in the Carlin trend occurred much earlier, possibly in the Early Cretaceous (about 117 Ma, Arehart et al., 1992, 1993c). However, the exact age of gold ore formation remains controversial, as indicated by Ilchick (1995, p. 208). Seedorff (1991) suggests that Carlin and similar deposits may actually be related to the onset of Basin and Range extension during the late Eocene to early Oligocene (42–34 Ma).

Several investigators have inferred a shallow epithermal origin for Carlin from the following types of evidence: (1) the characteristic epithermal suite of trace elements (Au, As, Sb, Hg, Tl) observed at many epithermal and hot spring deposits (Weissberg et al., 1979) and well developed at Carlin; (2) a maximum depth of 300 m for the Getchell orebodies inferred from geologic information, the vuggy character and ore-apex geometry, and a young age, no older than Pliocene (Joralemon, 1951, 1975); and (3) a maximum depth of 300 to 520 m at Carlin, based on boiling inferred from fluid inclusions (Radtke et al., 1980).

In contrast, Hardie (1966), Roberts et al. (1971), and Roberts (1986) estimated that at least 520 to 910 m of cover were above the ore zones at Carlin during ore formation. The deep ore in the Post-Betze area 10 km northwest of Carlin (Bettles, 1989) and near the Gold Quarry mine (Rota, 1987) as well as the deep ores at the Getchell mine discussed by Berger (1985) and the newly discov-

0361-0128/95/1654/0003-20$4.00

ered deep ores at the Rabbit Creek deposit (Parratt and Bloomstein, 1989) indicate that a relatively shallow geologic setting is not required for Carlin-type gold mineralization.

Based on a revised paragenetic framework (Kuehn and Rose, 1986, 1992) as well as prior and new fluid inclusion and stable isotope data at Carlin, this study focuses on reevaluation of the P-T-X constraints attending gold ore formation at Carlin and, by inference, similar sediment-hosted gold deposits. The inferred geologic setting of ore formation is then discussed. Specifically, the necessary minimum depths and geochemical processes leading to gold deposition at Carlin in a deep geologic setting of probable throttling and fluid mixing are contrasted with earlier shallow epithermal hot spring models.

Paragenetic Framework at the Carlin Deposit

Several characteristics of the Carlin deposit inhibit the development of a paragenetic sequence. The sedimentary host rocks have undergone diagenesis and multiple alteration events including weathering, so that not all rock-altering events are attributable to the Au-mineralizing event(s). The lack of obvious through-going and crosscutting veinlets, the restriction of many veinlet types to either the hanging wall or footwall, and the inability to observe gold visually inhibit conventional paragenetic interpretation. Probably because of these problems, little agreement exists on paragenesis at Carlin.

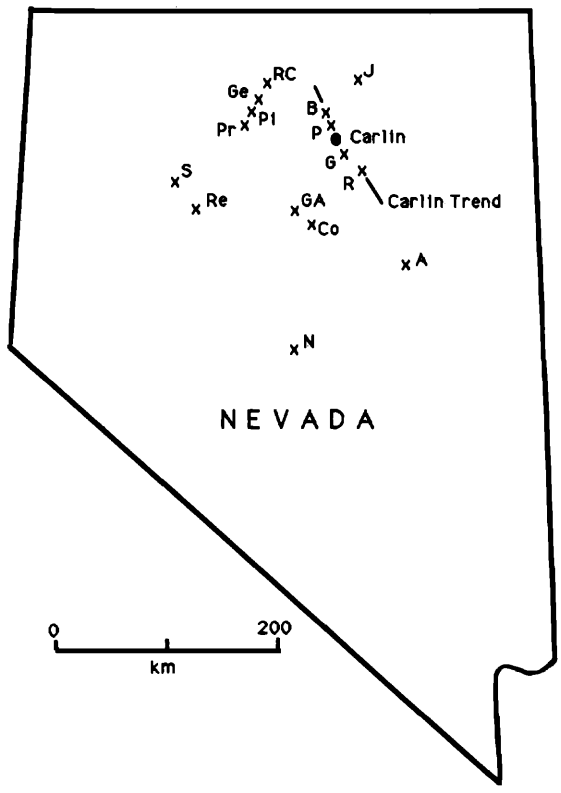

FIG. 1. Location of Carlin and similar gold deposits in Nevada. A = Alligator Ridge, B = Bootstrap, Co = Cortez, G = Gold Quarry, GA = Gold Acres, Ge = Getchell, J = Jerritt Canyon, N = Northunberland, P = Post-Betze, Pi = Pinson, Pr = Preble, R = Rain, RC = Rabbitt Creek-Chimney Creek, RE = Relief Canyon, S = Standard.

Previous work

Hausen (1967) discussed the paragenesis at Carlin as three separate general events: (1) Cretaceous barite and base metal mineralization, (2) Tertiary gold and associated As-Sb-Hg-Tl mineralization, and (3) Recent supergene effects. Dickson et al. (1979) discuss four separate disseminated and vein assemblages involving quartz, barite, Au, and rare Tl-As-Sb-Hg sulfide and sulfosalt minerals; however, only scant information is provided on the relative timing of these features. Radtke et al. (1980) present schematic diagrams of the Carlin paragenesis which define four stages in which different types of veinlets developed as a result of the introduction or removal of components from the ore zone and altered rocks. A given vein type or mineral assemblage was not necessarily restricted to a single paragenetic stage in this schematic approach nor is the relative timing of different veinlet types distinguished on the basis of crosscutting relationships. Bakken and Einaudi (1986) discuss at least nine different ages of veinlets labeled "types A through I" from oldest to youngest and describe the spatial relationship of these veinlets to mineralization and alteration in the Main Pit at Carlin. A paragenetic scheme consisting of "stages 1 to 5" is presented by Madrid and Bagby (1986, 1988) and was developed from crosscutting relationships exposed south of the Carlin mine and at the Preble, Pinson, and Bootstrap deposits.

Based on detailed field and laboratory studies (Kuehn, 1989; Kuehn and Rose, 1986, 1992), three major episodes can be distinguished, related to (1) hydrocarbon maturation, (2) gold ore deposition and associated alteration, and (3) oxidation (Table 1). These episodes are essentially unrelated temporally.

In more detail, the numerous types of veins or veinlets labeled A through F, can be divided into a series of stages defined largely on crosscutting relations. These stages are also distinguished by significant changes in fluid characteristics preserved in inclusions and stable isotope signatures. The observations listed do not exhaust the entire range of veinlet types or alteration features at Carlin. However, prior and future observations should fit into this general framework. Within a given stage, crosscutting relationships between different veinlets can be numerous and complex. For additional details on veinlets and typical samples, see Kuehn (1989).

Veinlets predating gold mineralization

Vein group A: Hydrocarbon stage (HC): All veinlet types of the early hydrocarbon (HC) stage contain high bulk density CH_4 fluid inclusions that coexist with a saline aqueous brine (Kuehn, 1989; Kuehn et al., unpub. data). Although production of CH_4 by the thermal maturation of organic matter must have occurred over a relatively long period of geologic time, reservoir conditions of 0.6 to 1.4 kbars at 155° ± 20°C are recorded in the countless crosscutting planes of secondary CH_4-rich fluid inclusions.

Carbon-rich zones are cut by dikes at several locations in the mine and at no scale do HC stage veinlets cut the dikes. HC stage veinlets are cut by all other veinlet types and also contain secondary inclusions of fluids typical of later veinlets of the paragenesis. Veinlets described by

TABLE 1. Paragenetic Framework for Fluid Evolution at the Carlin Deposit

Observation	Vein group	Stage	Fluids	Episode
Travertine, hyaline opal Stibiconite, sulfur Fe oxide on fractures Calcite with Fe oxide Peach-colored calcite Oxidation of pyrite, tan color Carbon removal	F	Oxidation (OX)	Temperature low (40°–140°C?) Oxidizing Deep weathering	Post-gold
Calcite veinlets Barite, calcite, quartz in vugs in jasperoid Massive white barite with minor stibnite Orpiment-calcite-barite-realgar-stibnite Calcite-realgar veins Calcite ± Fe dolomite veins	E	Late gold ore (LGO)	Salinity < 1.5 wt % NaCl equiv Temperature > 150°–220°C Low dissolved gas Non-boiling Non-evolved meteoric	Gold ore
Gas-poor quartz crystals Gas-rich quartz crystals Jasperoid breccias and stockwork veins Large-scale carbonate removal and progressive silicification, local jasperoid formation and extensive dike alteration	Dgp Dgr	Main gold ore (MGO)	Salinity 3 ± 1 wt % NaCl equiv Temperature 215° ± 30°C Immiscible CO_2-H_2O High-density CO_2 with H_2S	
Quartz veinlets with CO_2-rich fluid inclusions cut jasperoids and argillically altered dikes	C			
Igneous dikes cut carbon zones				
Local pyrobitumen veinlets cut early barite (rare) Sheared grayish barite veins with minor galena and sphalerite	B	Barite-base metal (BBM)	Salinity 9.7 to 16.7 wt % NaCl equiv	Pre-gold
White calcite ± euhedral quartz Brecciated pyrobitumen-calcite Quartz-calcite-pyrobitumen veins Dark calcite-carbon stylolites	A	Hydrocarbon (HC)	High-density CH_4 with CO_2, H_2S Salinity > 16 wt % NaCl equiv Immiscible CH_2-H_2O	

Bakken and Einaudi (1986) as types A and B as well as black quartz (Rota, 1987) at the Gold Quarry deposit are included in the HC stage.

Vein group B: Early barite ± base metal (BBM) stage: Massive, sheared grayish barite veins up to 3 m in width occupy several steeply dipping north-south- and north-northeast-striking structures in the Main and East Pits at Carlin (Radtke, 1985; Bakken and Einaudi, 1986). Several of these structures are also occupied by sheared and altered dikes. In contrast to later barite veins and vug-filling crystals, these early barite veins typically contain small elongate blebs of sphalerite and galena and give off a distinct fetid odor when outcrops are struck by a hammer or samples crushed in the laboratory.

Although Radtke et al. (1980) suggest that Cu-Pb-Zn mineralization occurred after the introduction of gold, and Bakken and Einaudi (1986) assign type I barite-sphalerite-galena veins to a late stage in the paragenetic sequence, the following observations suggest that barite ± base metal veins predate Au-As-Sb mineralization and, as initially suggested by Hausen (1967), are an early feature:

1. Some barite veins are cut by hydrocarbon veinlets and have bituminous residues within fractures (Hausen, 1967, p. 38, 124; Hausen and Kerr, 1968, p. 930; Hausen and Park, 1986, p. 122).
2. Barite ± base metal veins are crosscut by jasperoidal silica veinlets associated with gold mineralization; clasts of early barite are included in mineralized jasperoid breccias.
3. Saline aqueous fluid inclusions occur in barite associated with base metal sulfides (sample C85-004; Radtke, 1985, p. 101, samples 3512-M and 5109-J); crushing tests in kerosene reveal CH_4 with high internal pressure.
4. Primary base metal sulfides are commonly rimmed and/or replaced by As ± Sb-bearing base metal sulfosalts (jordanite, boulangerite, gratonite, tennantite, and tetrahedrite; Hausen, 1967; Radtke, 1985), suggesting that As ± Sb-bearing fluids postdate the base metal sulfides.

A second type of early veinlet also contains minor barite but lacks base metals and consists mainly of cream and white interlocking crystals of calcite, dolomite, and quartz. These veinlets are similar to the type E veins of Bakken and Einaudi (1986). Crushing studies in kerosene revealed high bulk density CH_4 fluid inclusions in these veins.

These observations define the barite ± base metal stage of mineralization at Carlin.

Veinlets temporally related to gold mineralization and alteration

Diagenetic and hydrothermal activity predating gold mineralization is delimited from gold mineralization and

accompanying carbonate removal and silicification by series of dikes which cut the carbon-rich zones after the introduced mobile organic matter had already thermally matured to solid pyrobitumen (Kuehn, 1989; Kuehn et al., unpub. data). These dikes are in turn severely altered and locally mineralized by the gold-bearing hydrothermal fluids (Kuehn and Rose, 1992). Clasts of altered dike material are included in mineralized jasperoidal breccias at Carlin and at the Bootstrap mine. Consequently, all features which cut the dikes and subsequent jasperoids must at least be considered as potentially related in time to gold mineralization.

Vein group C: Main gold ore (MGO) stage—quartz veins associated with dikes: Milky white quartz veins up to 6 cm wide cut and occur along the contacts of the intensely altered portions of dikes. The quartz typically has a greasy luster and releases copious gas on crushing. Severely altered zones contain anastomosing networks of milky white and turbid gray quartz veinlets with pyrite. This quartz contains low-salinity aqueous fluid inclusions as well as high-density CO_2-bearing inclusions (Kuehn, 1989, appendix D).

Vein group Dgr: Main gold ore (MGO) stage—gas-rich jasperoids and quartz vein stockworks: Stockworks of innumerable crosscutting milky white and gray translucent quartz veinlets are developed in jasperoids at Carlin (Fig. 2A). Each of these veinlets contains numerous planes of secondary high bulk density CO_2 fluid inclusions lacking appreciable CH_4. These jasperoids with quartz vein stockworks are spatially associated with Au mineralization and exposed in the south walls of the East Pit (Kuehn and Rose, 1992), the Main Pit (Bakken and Einaudi, 1986), and the West Pit (Radtke, 1985). Structurally controlled jasperoids acted as feeders to stratiform jasperoids and these same intensely silicified areas were subsequently laced with milky white and gray translucent stockwork quartz veinlets (Fig. 2C). Unoxidized intensely silicified areas locally contain pyrite and stibnite in these veinlets.

Crushing of these quartz veinlet stockworks consistently releases gases under high internal pressures. Although the inclusions are too small for quantitative studies (typically <1–3 μm), low-temperature petrography confirms that many dark, one-phase fluid inclusions at 25°C are actually liquid CO_2. Several samples also contain three-phase fluid inclusions at room temperature as previously described (Nash, 1972; Radtke, 1985).

High bulk density CH_4-rich or saline aqueous inclusions typical of the early HC stage are lacking in quartz from stockworks, even though the quartz contains thousands of planes of secondary fluid inclusions. This observation demonstrates that these quartz veinlets formed under conditions significantly different from and distinctly later than HC stage fluids. Because these milky white and gray translucent quartz veinlets are intimately associated with jasperoid development spatially related to gold mineralization, these veinlets are assigned to the MGO stage.

Jasperoidal silica breccia veinlets (Fig. 2F) and veinlet stockworks of dark gray to black, sugary-textured jasperoidal silica in footwall rocks also represent MGO stage silicification. Although this replacement-type silica rarely contains fluid inclusions, these jasperoid veinlets are intimately associated with the gray translucent and milky white quartz veinlets discussed above and have similar oxygen isotope signatures. When developed in zones previously occupied by HC stage veinlets, these jasperoidal silica breccia veinlets crosscut and entrain clasts of earlier HC stage CH_4-bearing quartz.

Alteration of calcareous siltstones at Carlin consists of successive zones of calcite dissolution, dolomite dissolution, and conversion of illite to kaolinite-dickite, zoned around faults and permeable beds interpreted as feeders for the Au mineralization (Kuehn and Rose, 1992). This alteration is inferred to result from the acid conditions imparted by high CO_2 in the hydrothermal fluid, and therefore is correlated with the Dgr veins.

Quartz-bearing veins described by Bakken and Einaudi (1986) as types G and H are similar to our MGO stage silicification features; their type F veinlets may represent MGO stage or earlier siliceous replacement of diagenetic and HC stage features.

Vein group Dgp: Main gold ore (MGO) stage—gas-poor quartz veinlets and selvages: Several samples of quartz veinlets and selvages are similar in occurrence and habit to Dgr quartz but lack the high bulk density CO_2- and CH_4-rich inclusions typical of earlier vein types even though they contain numerous planes of secondary fluid inclusions (Fig. 2D and E). This gas-poor quartz is similar isotopically to jasperoid and Dgr quartz, and therefore is termed to the Dgp group.

Vein group E: Late gold ore (LGO) stage: A series of different vein types characterize the later and more peripheral phases of gold mineralization (Table 1). The strong correlation of Au with As and Sb at Carlin (Hausen, 1967; Akright et al., 1969; Radtke et al., 1980; Evans and Peterson, 1986; Arehart et al., 1993a) indicates that these veins are indeed part of the gold ore episode. These group E veinlets cut both mineralized and altered rocks, and some of them constitute ore themselves. The open-space mineral deposition and vuggy character of several group E veinlet types also contrast with the group C and D veinlets.

Crushing of mineral separates from group E veinlets revealed mild bubble expansion in some cases but never the violent expansion typical of earlier gas-rich stages of the paragenesis. Inclusions in group E veinlets contain a low-salinity aqueous fluid. Clathrate-melting temperatures confirmed that some inclusions contained at least minor amounts of dissolved gases.

The following vein types are recognized in group E: (1) orpiment ± calcite veins and breccia zones, (2) white calcite veins, (3) white calcite and realgar veins, (4) realgar ± barite and white calcite veins and coatings, (5) white barite ± stibnite veins with minor quartz, (6) quartz, barite, and calcite in vugs in jasperoid breccias, and (7) euhedral yellow barite, cinnabar, tetrahedrite, and pyrite in a matrix of dickite and quartz.

The white calcite veins (type 2 above) are the most abundant type. They define a broad halo of megascopic ore-related effects above and lateral to the ore, and occur less extensively below ore. The calcite is coarse grained, occurs in veins up to several centimeters thick, commonly shows growth inward toward the center of the vein, and

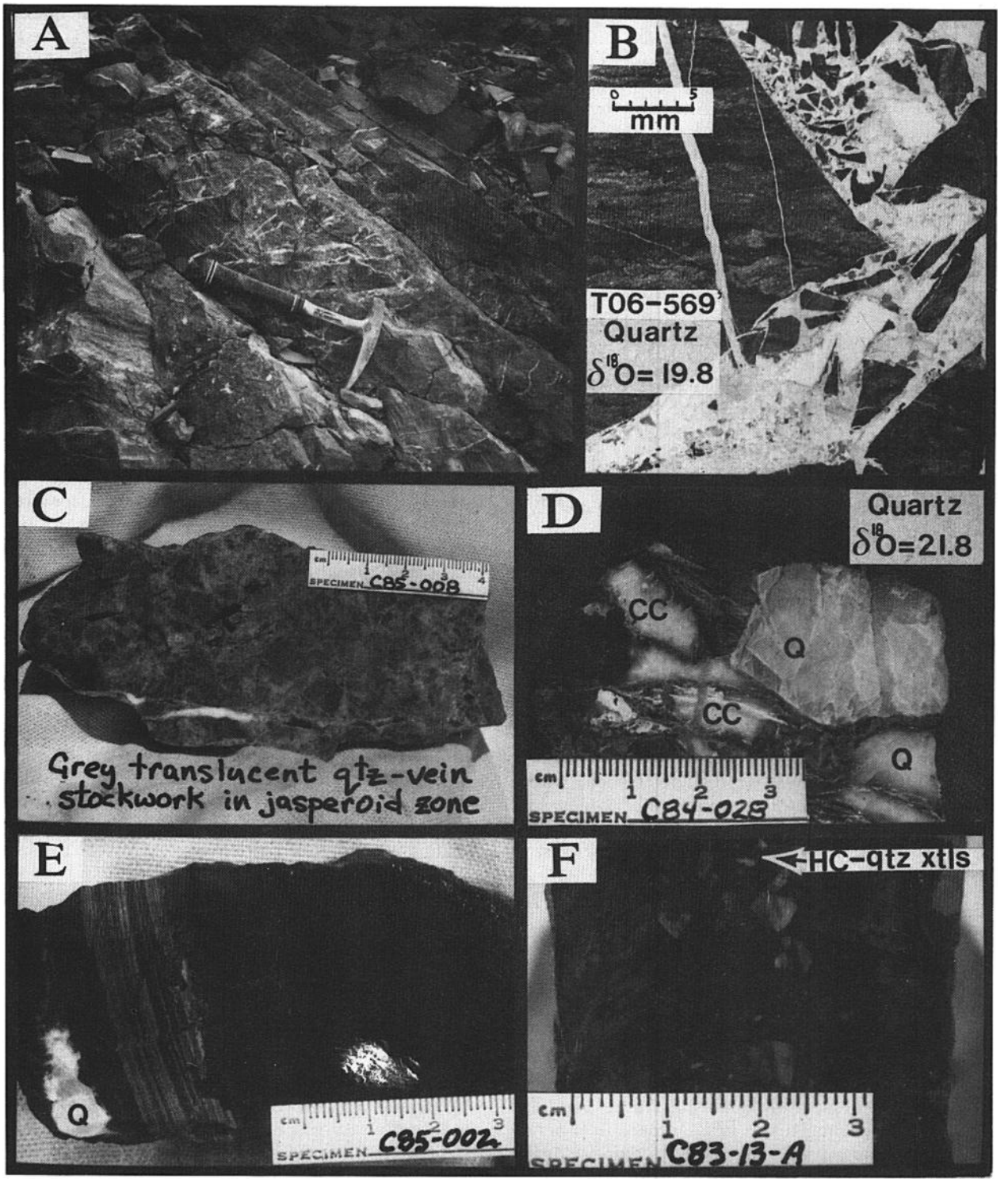

FIG. 2. Main gold ore stage silicification, quartz vein stockworks, and gas-free quartz crystals. A. Quartz vein stockworks in jasperoids from the 6640 level of the south wall of the Carlin West Pit (near sample 5630-J of Radtke, 1985, p. 101). B. Quartz stockwork breccia sample from leached footwall rocks; also contains dickite and clear to yellow anhedral barite crystals (elev 5,734 ft, N23807, E20329 in mine coordinates). C. Gray translucent quartz vein stockworks developed in northeast-striking, south-dipping mineralized jasperoid feeder zone from the 6120 level of the Main Pit at Carlin (N22729, E18831) described by Bakken and Einadi (1986, fig. 6D, p. 397). D. Milky white, gas-poor quartz (Q) with a greasy luster and lacking any evidence of high density CO_2 or CH_4 inclusions; revealed in HCl-etched sample of anasamosing calcite (CC) veinlets from the 6280 level of the Carlin East Pit (N42025, E20472). E. White, subhedral gas-poor quartz developed in selvage parallel to bedding in an area of high-grade gold mineralization on the 6180 level of the Carlin East Pit (N23408, E20372). F. Oxidized jasperoid breccia vein from the 6180 level of the Carlin Main Pit (N22770, E18920) developed in footwall of mineralization.

constitutes up to several percent of the rock. These veins correlate with the type C veinlets of Bakken and Einaudi (1986), the stage III (acid leaching and oxidation) calcite veins of Radtke et al. (1980), and the stage V calcite veins of Madrid and Bagby (1986, 1988). Although they appear visually similar to some quartz-poor HC stage veins, they lack CH_4 inclusions and contain only low-salinity aqueous inclusions.

Millimeter-sized euhedral quartz lining vugs in postjasperoidal breccia (type 6 above) is also common. This quartz is clear, rather than milky as in earlier stages, and lacks gas-rich inclusions. This type correlates with type H ore-stage silica of Bakken and Einaudi (1986).

The As- and Sb-bearing types are much more restricted in extent but have furnished much more spectacular samples and varieties of minerals. Age relations among veins within group E are conflicting or lacking because of the localized occurrence of these types.

Veinlets which postdate gold mineralization

Oxidation of the mineralized and altered rocks to a tannish-brown color occurred after the latest stage of widespread calcite veining, as shown by paragenetic relations, the presence of low-temperature Fe oxide (goethite), and other criteria (Kuehn and Rose, 1992). There is no direct correlation between the major stage of carbonate removal and the oxidation process (Kuehn and Rose, 1992). Other types of postgold veinlets are sparse clear calcite growing over Fe oxides, salmon to peach-colored calcite veinlets, a travertine vein in a mud and gouge-filled structure, alunite (Arehart et al., 1992), and local chalcedonic silica and hyaline opal. The latter may be related to present-day thermal waters such as those encountered near the Bootstrap and Goldstrike mines. Gold deposits near Carlin containing significant sinter are verifiably young and hosted in volcanic rocks (i.e., the Hollister deposit and USX orebody in the Ivanhoe district 8 km northwest of the Dee deposit).

Fluid Inclusion Studies and Thermobarometric Constraints

Carlin and other sediment-hosted deposits do not commonly provide material in which fluid inclusions can be clearly interpreted as primary. Most veinlet material appears cloudy and contains numerous planes of secondary inclusions. The general principle applied here is that later fluids are expected as secondary inclusions in earlier minerals, but not the reverse. Fluid inclusion studies reported here involved crushing tests, low-temperature petrography, and standard heating and freezing studies (Kuehn, 1989), as well as laser Raman microprobe analyses of selected inclusions using methods described by Pasteris et al. (1986). In addition, representative samples were analyzed for trace gases of individual inclusions using a rapid-scanning quadrupole mass spectrometric technique (Bendrick, 1989).

Types of fluid inclusions at Carlin

The wide variety of fluid inclusions in samples from the Carlin mine are grouped into 12 classes in Table 2. The classification is based on number and identity of phases at 25°C, and on bulk composition inferred from microscopic observations during heating and cooling. Their paragenetic occurrence is also summarized in Table 2, and must be interpreted with the proviso that many inclusions are secondary. Interpretations of hydrothermal conditions during the various stages, based largely on fluid inclusion data, are summarized in Table 3.

Many of the single-phase inclusions are filled with either high-density $CH_4 \pm CO_2$ which nucleates a bubble at < -82°C (type 1A, Table 2) or relatively CH_4-free $CO_{2(l)}$ which nucleates a vapor bubble at $T < 25$°C and shows triple-point melting near −56.6°C (type 1B, Fig. 3). A very small volume of $H_2O_{(l)}$ wetting the inclusion walls may also be present. Neither type 1A or 1B inclusions decrepitated upon heating to around 250°C, suggesting that total homogenization is to a CH_4- or CO_2-rich supercritical fluid at moderate temperatures.

Type 1C one-phase inclusions contain liquid H_2O which apparently was trapped at sufficiently low temperatures to preclude the nucleation of a vapor phase. Numerous type 1C inclusions were confirmed to be liquid water by the generation of a vapor bubble after stretching during freezing runs (Roedder, 1984), by laser Raman microprobe analysis, or by crushing tests without obvious bubble collapse.

Four varieties of H_2O-rich two-phase inclusions are present. Type 2A saline inclusions homogenize near 155° ± 20°C and are typical of the HC and possibly BBM stages of the paragenesis. Type 2B moderate-salinity H_2O-CO_2 inclusions generate $CO_{2(v)}$ upon cooling, homogenize between 130° and 280°C, and are present in MGO and earlier stages. Type 2C inclusions also contain $H_2O \pm CO_2$ as shown by clathrate formation; however, they fail to nucleate a readily apparent third fluid phase upon cooling. Type 2C inclusions are present in minerals of the LGO and earlier stages. Type 2D low-salinity aqueous inclusions homogenize over a wide range of temperature and are present in all samples but are dominant in LGO and younger stages of the paragenesis. All these types of two-phase H_2O-rich inclusions were apparently classified as "type I liquid rich" by Radtke et al. (1980).

A second major group of two-phase inclusions contains dominantly high-density $CO_{2(l)}$ at room temperature. Type 2E inclusions contain both liquid and vapor CO_2 in varying proportions and homogenize to $CO_{2(l)}$ between 25° and 31°C. Type 2F inclusions contain a small amount of $H_2O_{(l)}$ surrounding a large volume percent $CO_{2(l)}$ which nucleates a third phase, $CO_{2(v)}$, upon cooling below room temperature (Fig. 3). Type 2F inclusions lack low-density water vapor; however, at 25°C these inclusions meet the criteria of being type II vapor-rich as defined by Radtke et al. (1980).

Three varieties of fluid inclusions with three phases at 25°C (liquid H_2O, liquid CO_2, CO_2 vapor) were observed. Similar inclusions have been reported by Nash (1972) and Radtke at al. (1980). The most common is type 3A in which the two CO_2 phases homogenize to $CO_{2(l)}$ below 31°C. Type 3B is less common and contains two CO_2 phases that homogenize to $CO_{2(v)}$ below 31°C. Both type 3A and 3B varieties show final homogenization to $H_2O_{(l)}$ between 130° and 280°C, most commonly at 215°

TABLE 2. Major Types of Fluid Inclusions in Samples from the Carlin Gold Deposit, as Observed at 25°C

Type	Major contents	Comments	Stage[1] and veinlet group
1A	One-phase $CH_4 \pm CO_2$	Nucleates vapor bubble below −82°C	HC, BBM (A, B)
1B	One-phase CO_2, only trace CH_4	Triple point melting near −56.6°C	MGO (C, Dgr, E)
1C	One-phase H_2O	May nucleate vapor at low T	LGO (E, F)
2A	Two-phase $H_2O_{(l+v)}$	High-salinity $H_2O_{(l)}$, first-melting T very low	HC, BBM (A, B)
2B	Two-phase H_2O-rich with $CO_{2(l)}$	Generates $CO_{2(v)}$ on cooling	MGO (C, Dgr, E)
2C	Two-phase H_2O with low CO_2	Forms clathrate at low T_{CO_2}	MGO (C, Dgr, E)
2D	Two-phase $H_2O_{(l+v)}$, low salinity	No clathrate formed on cooling	LGO (E, F)
2E	Two-phase CO_2 rich with $CO_{2(l+v)}$	Homogenizes to $CO_{2(l)}$ at 25°–31°C, melts near −56.6°C	MGO (C, Dgr)
2F	Two-phase $CO_{2(l)}$ with minor $H_2O_{(l)}$	Generates $CO_{2(v)}$ on cooling, melts near −56.6°C	MGO (Dgr)
3A	Three-phase H_2O-rich $CO_{2(l+v)}$	CO_2 homogenizes to $CO_{2(l+v)}$	MGO (C, Dgr, E)
3B	Three-phase H_2O-rich $CO_{2(l+v)}$	CO_2 homogenizes to $CO_{2(v)}$	MGO (Dgr)
3C	Three-phase CO_2-rich, with minor $H_2O_{(l)}$	CO_2 phase homogenizes below 31°C	MGO (C, Dgr, E)

[1] Inferred main stages of formation; inclusions also commonly occur as secondary inclusions in earlier stages

± 30°C. Rare type 3C inclusions are CO_2 rich with minor H_2O, occur in MGO stage quartz, and behave similarly to CO_2-rich type 2E inclusions.

Fluids at Carlin prior to gold mineralization

For the HC stage, typical filling temperatures of brine inclusions and the P-V-T relations of the coexisting $CH_4 \pm CO_2$ mixture indicate P-T conditions around 155° ± 20°C and 0.6 to 1.4 kbars during or after the formation of these early veins (Kuehn, 1989; Kuehn et al., unpub. data). Homogenization and ice-melting temperatures for inclusions in HC, MGO, and LGO stage veinlets (Fig. 4) clearly demonstrate the absence of the early brine ($T_{m_{ice}} < -10$°C) in MGO and later stages of the paragenesis as well as the presence of secondary aqueous fluid inclusions with MGO and LGO stage characteristics in the early HC stage veinlets.

Both type 1A high-density CH_4 and type 2A saline aqueous inclusions were observed in several BBM stage samples, and pyrobitumen veinlets locally cut BBM stage veins (Hausen, 1967). These observations indicate a close relationship in time and depth to the HC stage. Radtke et al. (1980) report salinities in liquid-rich inclusions from samples which also contained base metal sulfides (5109-J and 3512-M) ranging from 9.7 to 16.7 wt percent NaCl equiv. Homogenization temperatures in these Radtke samples generally were higher than 225°C and consistent with sulfur isotope fractionations of barite-sphalerite and barite-galena pairs yielding temperatures between 250° and 305°C (Radtke et al., 1980).

Fluids during the main and late gold ore stages at Carlin

The main inclusion assemblage in group C quartz is CO_2 rich and similar to that found in group D quartz veinlets cutting jasperoids. Minor to moderate CH_4 in some inclusions may have resulted from cracking of relatively ma-

TABLE 3. Synopsis of Fluid Characteristics of Major Stages of the Carlin Paragenetic Framework

Fluid characteristics and constraints	Hydrocarbon (HC) stage	Main gold ore (MGO) stage	Late gold ore (LGO) stage	Late oxidation (OX) stage
Age estimates	Pre-Early Cretaceous (>120 Ma)	Early Cretaceous	(~120 Ma)	Tertiary to Recent
Temperature (°C)	155 ± 20	215 ± 30	175–250 (?)	Probably < 150
Pressure	0.6–1.4 kbars	800 ± 400 bars	Undefined	Probably low
Salinity (wt percent NaCl equiv)	Ca. 16 ± 4	Ca. 3 ± 1	<1.5?	Probably very low
Immiscible conditions	Yes: CH_4-H_2O	Yes: CO_2-H_2O	No	No
Evidence	High-density CH_4	High-density CO_2		
Major and trace gases present	Major CH_4; minor CO_2, H_2S	Major CO_2 with H_2S; minor CH_4 (SO_2?)	Minor CO_2; trace H_2S, SO_2	Virtually absent
$\delta^{18}O$ of fluid reservoir (‰)	8–13	5–9	<−4 to −3	Probably near 0.0
δD of fluid reservoir (‰)	~9; connate water?	Inclusion fluids: −87 to −153; kaolinite: −161	Inclusion fluids: −139 to −149	Undetermined
Control on ^{13}C	Country-rock carbonates	Country-rock carbonates	Country-rock carbonates	Partly organic matter
Calcite range (‰)	(−1.0 to +2.1)	(−1.6 to 0.1) Possibly $C_{organic}$	(−1.6 to +2.0)	(−7.6 to −4.6)
Probable origin	Connate brine	Evolved meteoric water plus deep volatiles, Au	Meteoric water	Meteoric water?

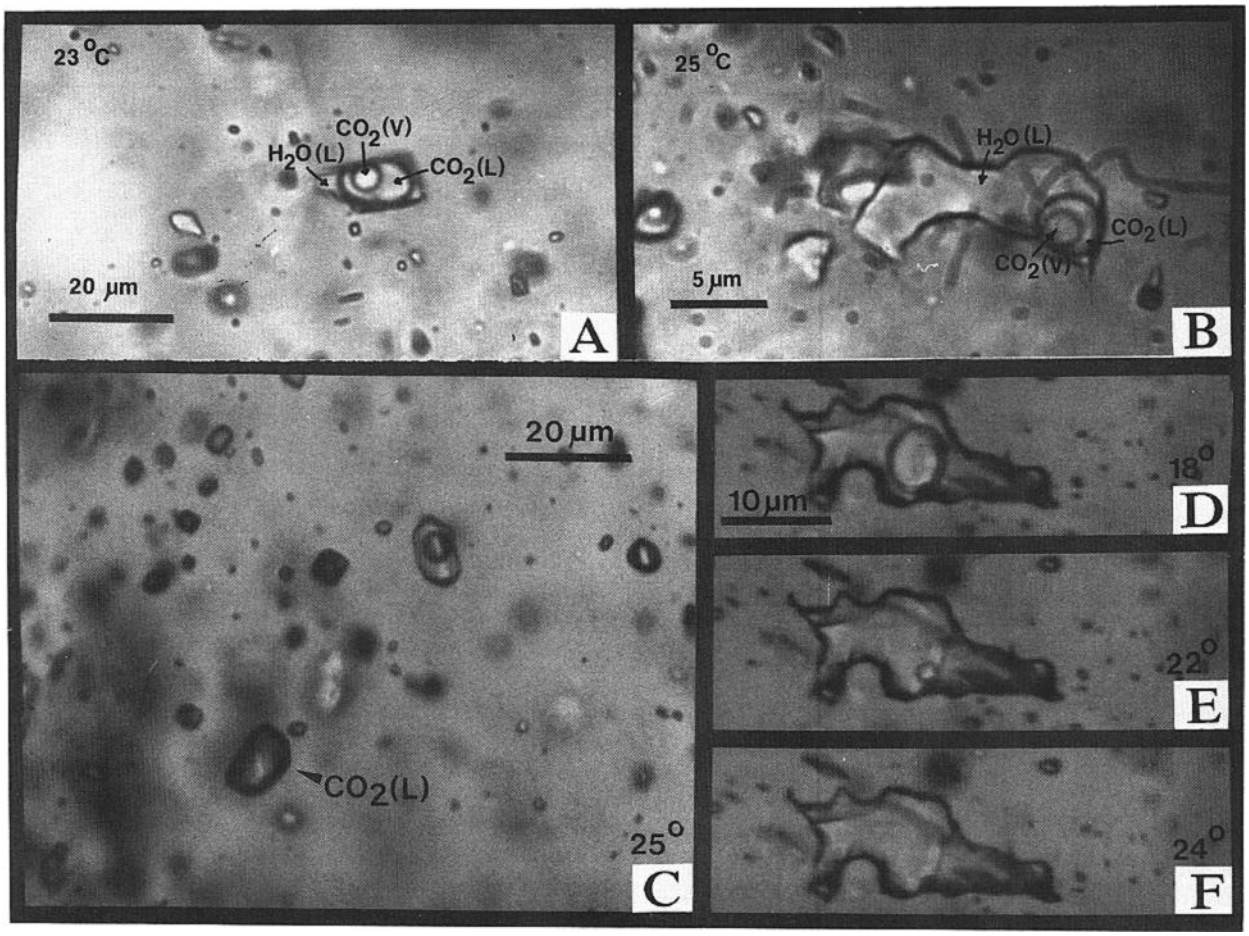

FIG. 3. High-density CO_2-rich fluid inclusions typical of MGO stage (group Dgr) samples and containing either one, two, or three phases at 25°C. Samples C83–036 and C83–009. Inclusions shown in A and B are also described in Pasteris et al. (1986). A. CO_2-rich inclusion at 23°C which is two-phase at 25°C and nucleates a third central $CO_{2(v)}$ phase with less than 2°C of cooling. Total homogenization is to the CO_2 phase. B. Three-phase fluid inclusion at 25°C where the two central CO_2 phases homogenize to the $CO_{2(l)}$ phase prior to 31°C; total homogenization is to the H_2O phase around 240°C. C. Coexisting H_2O-rich and CO_2-rich inclusions in the same field of view representing opposite sides of the CO_2-H_2O solvus. Dark CO_2-rich inclusion appears to contain only one phase at 25°C; upon cooling, a $CO_{2(v)}$ bubble nucleates at around 11°C. D–F. This large CO_2-rich inclusion appears to contain only one phase at 24°C (D) although a small amount of water probably wets the inclusion walls. At 18°C (E) a $CO_{2(v)}$ bubble is present which shrinks and disappears upon warming to 24°C (F).

ture bitumen at high temperatures adjacent to the dikes, possibly accompanied by thermal decomposition of carbonate wall rock to furnish the CO_2. Because it is unlikely that all the abundant CO_2-rich inclusions in group C quartz veins are secondary and much later than the sparse CH_4-rich inclusions in this same quartz, the typical CO_2-rich fluids like those in group D were probably present during the formation of group C veins.

Jasperoidal silica breccia veinlets are usually devoid of inclusions; however, the commonly associated gray translucent and milky white MGO stage quartz contained various combinations of nearly CH_4-free, H_2O-CO_2 inclusions of types 1B, 2B, 2E, 2F, and 3A-C (Fig. 3). The $H_2O \pm CO_2$ inclusions preserved in MGO stage veinlets homogenize over a wide temperature range, with a median homogenization temperature ($Th_{(l)}$) of about 215°C and an ice-melting temperature ($T_{m_{ice}}$) of about −3°C (Fig. 4). Although these inclusions represent primary and secondary MGO and LGO stage fluids, the majority have distinctly lower $T_{m_{ice}}$ than inclusions in LGO stage quartz (median $T_{m_{ice}}$ about −1°C), and are taken to represent MGO stage fluids.

Because some inclusions in HC stage veinlets have $Th_{(l)}$ an $T_{m_{ice}}$ values similar to inclusions in MGO stage veinlets (Fig. 4), these inclusions in HC stage quartz may be secondary inclusions containing MGO stage fluids. However, the inclusions with lower $T_{m_{ice}}$ values (<4°C, filled symbols in Fig. 4) might represent either fluids of the BBM stage, or saline HC stage inclusions opened and diluted with later, less saline MGO stage and/or LGO stage fluids (Sterner and Bodnar, 1989). Because of the small scatter and the overlap with MGO stage inclusions, the intermediate-salinity inclusions are considered more likely to represent either the main gold ore or BBM stages.

The ubiquitous presence of LGO stage and later fluid inclusions in all MGO stage samples and the lack of adequate data for the system H_2O-CO_2-NaCl make constraining P-T-X conditions during the MGO stage difficult. In

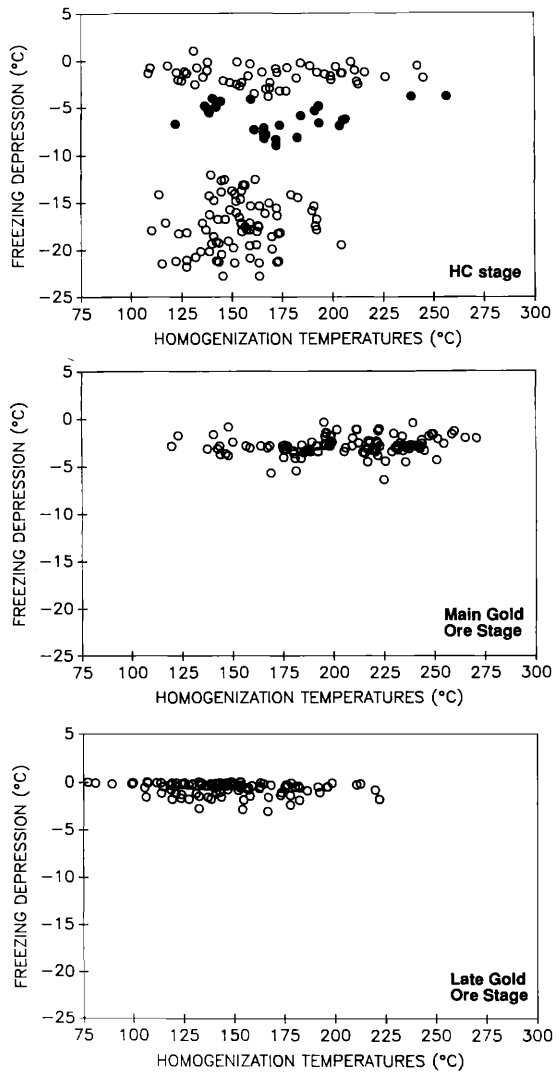

FIG. 4. Comparison of aqueous fluid inclusion data for the Carlin deposit. Top: Premineralization HC stage veinlets. Middle: MGO stage quartz veinlet (groups C and D). Bottom: LGO stage veinlets. Intermediate apparent salinity fluids shown by filled circles on the HC stage diagram are absent in LGO stage veinlets and possibly represent either MGO stage fluids, BBM stage fluids, or both.

addition, although the cloudy MGO stage material contained a myriad of 1- to 3-μm-diam inclusions, they were typically too small to work with and commonly only a few inclusions per sample yielded quantitative data. Figure 5 shows a compilation of homogenization temperatures for aqueous inclusions from quartz of the main gold ore stage (groups C, Dgr, and Dgp). Evaluation of temperatures during MGO stage time must consider (1) leakage to create erratic higher values, (2) secondary trapping of low-salinity LGO stage and later fluids, and (3) trapping of MGO stage fluids in a one-phase condition requiring a pressure correction. With these caveats in mind, based on the average value and large population variance, the best estimate of the minimum temperature during MGO stage time at Carlin is 215° ± 30°C.

Although the CO_2-rich inclusion types 2E and 2F, and the closely related types 1B and 3C, exhibit a wide range of characteristics at 25°, all could result from trapping in a limited range of P-T-X conditions (Connolly and Bodnar, 1983). All four varieties of high-density CO_2-rich inclusions are thought to represent the CO_2-rich side of the H_2O-CO_2(± NaCl) solvus (Roedder and Bodnar, 1980; Pichavant et al., 1982; Ramboz et al., 1982; Bodnar et al., 1985). The temperatures and modes of homogenization of the two CO_2 phases in these CO_2-bearing fluid inclusions provide constraints on trapping pressures at Carlin during the MGO stage. These pressure estimates are only approximate minimum values because (1) the H_2O-CO_2 solvus for temperatures between 180° and 250°C is not very sensitive to pressure and the CO_2 content of the bulk fluid cannot be determined accurately, (2) the solvus in the system CO_2-H_2O expands greatly in the presence of even small amounts of dissolved components such as NaCl (Gehrig, 1980), and (3) other gases (CH_4, H_2S, and SO_2) could significantly affect the P-V-T-X properties of the fluid; however, in most samples, the trace amounts detected by mass spectrometry probably have little effect (Diamond, 1994).

For CO_2-rich MGO stage inclusions of types 1B, 2E, 2F, and 3C in which CO_2 phases are observed to homogenize to $CO_{2(l)}$ between 10° and 31°C and final T_h values are 180° to 250°C, the required trapping pressures range from 400 to 1,400 bars (Fig. 6A). The H_2O-rich type 2B and 3A inclusions which have an observed CO_2 homogenization to $CO_{2(l)}$ between 20° and 31°C require pressures from 750 to 1,700 bars. The H_2O-rich type 3B inclusions that homogenize to $CO_{2(v)}$ between 25° and 31°C require pressures from 300 to 750 bars. Type 2B and 3A inclusions are much more common than type 3B and could give rise to this latter type with minor amounts of stretching or leakage. In contrast, no post-trapping effects could generate type 2B or 3A inclusions from fluids of compositions and densities that would naturally give rise to type 3B inclusions.

Salting out of CO_2 from the aqueous phase could significantly affect the calculated CO_2 homogenization temperatures shown in Figure 6A by increasing the effective bulk density of the free CO_2 in the inclusion (Bodnar et al., 1985). Because of the small volume percent $H_2O_{(l)}$ in CO_2-rich type 1B, 2E, 2F, and 3C inclusions, these effects are much less severe. Consequently, the high-density CO_2-rich inclusions representing the CO_2-rich side of the H_2O-CO_2 (± NaCl) solvus provide the best estimate of minimum trapping pressures, 800 ± 400 bars.

Up to 2.43 mole percent CO_2 can remain dissolved in the aqueous phase without generating a separate CO_2 liquid phase at 25°C (Bodnar et al., 1985). At room temperature these inclusions would have an internal pressure of 64 bars and appear as H_2O-rich types 2C or 2D. Higher CO_2 contents are required for type 3B inclusions, and minimum CO_2 contents of around 5 to 10 mole percent CO_2 can be estimated using CO_2/H_2O volume ratios of H_2O-rich type 2B and/or 3A inclusions (Bodnar et al., 1985). Depending on the effects of dissolved NaCl and other components, the actual amount of CO_2 may be somewhat lower.

Coexisting H_2O-rich (types 2B, 3A, 3B) and CO_2-rich (types 1B, 2E, 2F, 3C) inclusions suggest that two-phase

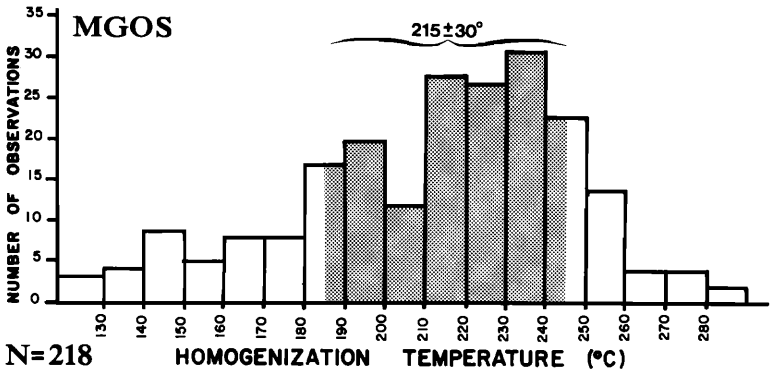

FIG. 5. Histogram of homogenization temperatures of aqueous fluid inclusions in samples from veinlet groups C, Dgr, and Dgp. Average value and one standard deviation are highlighted.

conditions are recorded during at least portions of MGO stage time. These immiscible conditions, and in particular, the existence of CO_2-rich inclusions, constrain both P and T during MGO stage time to 800 ± 400 bars and 215° ± 30°C (Fig. 6A).

Only minimum estimates of temperature are provided by fluid inclusions in LGO and later stages because only type 2C, 2D, and 1C low-salinity H_2O-rich inclusions are present. However, as shown in Figure 6B, the isochores for type 2D inclusions homogenizing at 150° to 220°C (avg 180°C) project into the same 0.5- to 1.0-kbar region where fluids containing 5 to 10 mole percent CO_2 would be in a one- or two-phase condition and could generate type 2B inclusions. Figure 6B also shows that for a given T and CO_2 content, a drop in pressure would result in a two-phase condition which could give rise to coexisting H_2O-rich type 2B, 3A, and 3B and CO_2-rich type 1B, 2E, 2F, and 3C inclusions.

Additional constraints on maximum temperatures at Carlin: Three separate observations constrain maximum temperatures during or after gold mineralization at the Carlin deposit. First, all samples of purified realgar from LGO stage veinlets throughout the ore zone and hanging wall show clean alpha-AsS X-ray diffraction patterns, providing an upper temperature limit of around 265° ± 5°C (Hall and Yund, 1964). Second, the melting points of ellisite (Tl_3AsS_3) at 325°C, lorandite ($TlAsS_2$) at 292°C, and orpiment (As_2S_3) at 311°C also provide upper limits on temperature (Dickson et al., 1979).

Finally, both Ar^{40}/Ar^{39} measurements on K mica separates from propylitically altered dike material (Kuehn, 1989) and conventional K/Ar measurements on mineralized sedimentary rocks from Carlin (W.C. Bagby and W. Pickthorne, pers. commun., 1984) show only minimal resetting due to later thermal events. Burton et al. (1985) found similar results for mineralized samples from the Jerritt Canyon, Sterling, Getchell, and Alligator Ridge deposits. In contrast, Arehart et al. (1993c) and Osterberg (1989) found appreciably reset ages in certain samples from the Post-Betze and Chimney Creek gold deposits. In order for fine-grained K mica to recrystallize and/or to lose appreciable Ar, temperatures must exceed about 250°C for a significant period of time, based on studies of metamorphic rocks (McDougall and Harrison, 1988).

These three separate lines of evidence suggest that temperatures during MGO and LGO stage deposition at Carlin probably did not exceed 250° to 265°C for extended periods of time, in agreement with the fluid inclusion data for MGO and LGO stage veinlets suggesting that temperatures were dominantly 215° ± 30°C.

Trace gas studies of Carlin fluid inclusions

Thirty representative samples were analyzed for water and trace gas components in thermally decrepitated individual inclusions using a mass spectrometric technique (Barker and Smith, 1986; Bendrick, 1989). Reported data assume that all components are equally sensitive, which is probably not exactly correct. Therefore, attention should be focused on differences between samples, rather than on absolute ratios or absolute quantities.

Figures 7 and 8 summarize the changes in relative amounts of CH_4, CO_2, H_2S, and SO_2 through the paragenesis. Because all inclusions in each sample are analyzed and reported in Figure 8, older stages of the paragenesis may contain gases from secondary inclusions, which cannot be distinguished from primary inclusions in this method. The apparently high CO_2 content recorded in the BBM stage may be such an example.

Hydrogen sulfide values are highest in the BBM stage, probably derived by thermal cracking of kerogen (Tissot and Welte, 1984) or by thermochemical SO_4 reduction by organic matter during late catagenesis and metagenesis. Maximum H_2S concentrations occur at depths between 3 and 5 km (Tissot and Welte, 1984, p. 455), corresponding well with the 2.5- to 5.8-km constraints independently provided by HC stage fluid inclusion data (Kuehn, 1989).

The significant amounts of H_2S and SO_2 detected in both MGO and LGO stage samples are not readily discernible with conventional fluid inclusion techniques. Laser Raman microprobe studies have also detected H_2S in individual CO_2-rich MGO stage fluid inclusions at Carlin (Pasteris et al., 1986). The trace gas studies at Carlin clearly show high CO_2/CH_4 ratios as well as the presence of H_2S and oxidized sulfur gases (SO_2) during the MGO and LGO stages.

Salinities of Carlin fluid inclusions

The $T_{m_{ice}}$ values (Fig. 4) can be interpreted only as maximum apparent salinities because of the possible effect of

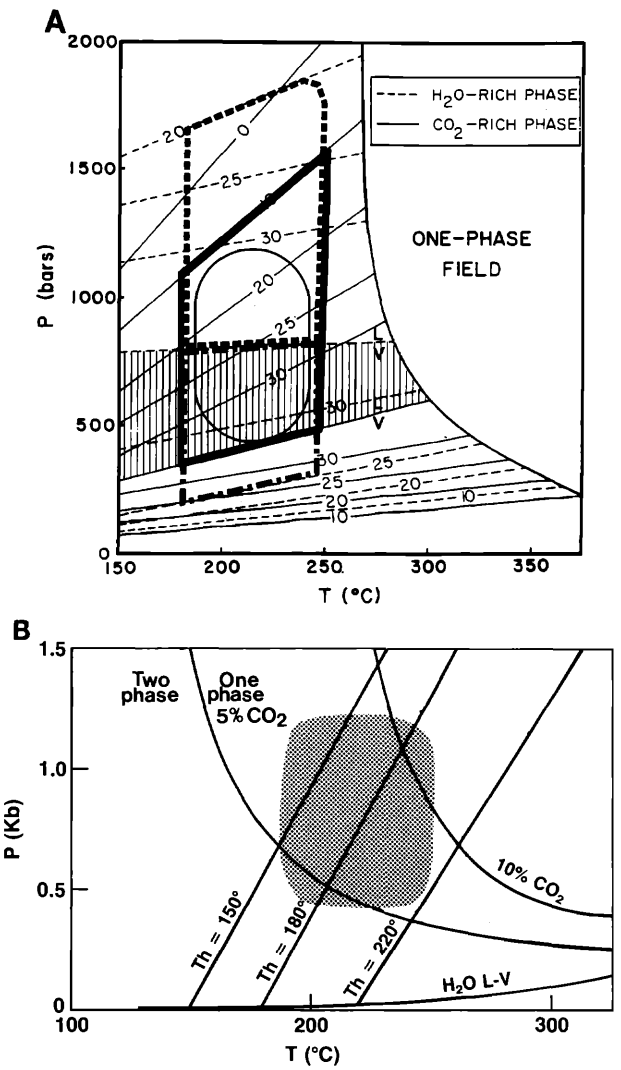

FIG. 6. A. Calculated homogenization temperatures (T_h) and phase relations (light solid and dashed lines) for the two CO_2 phases in H_2O-CO_2 fluid inclusions for a range of trapping conditions, plus interpretation of trapping conditions at Carlin. L/V = critical isotherms (31°C) for both types of inclusions. Vertical pattern = area between these critical isotherms. If $P_{trapping}$ lies above the critical isotherm, then the two CO_2 phases homogenize to $CO_{2(l)}$, and conversely, below it to $CO_{2(v)}$. Bold dashed line = H_2O-rich type 3A and 2B inclusions with final T_h values of 215° ± 35°C and $T_{h_{CO_2}}$ to $CO_{2(l)}$ of 20° to 31°C. Bold dash-dot line = H_2O-rich type 3B inclusions with final T_h values of 215° ± 35°C and $T_{h_{CO_2}}$ to $CO_{2(v)}$ of 25 to 31°C. Bold solid line = CO_2-rich type 1B, 2E, 2F, and 3C inclusions with $T_{h_{CO_2}}$ to $CO_{2(l)}$ of 10° to 31°C and final CO_2-H_2O homogenization values of 215° ± 35°C. Oval line = approximate P-T conditions where drops in pressure would result in immiscible conditions and could develop the observed MGO stage and LGO stage assemblages of coexisting H_2O-rich and high bulk density CO_2-rich inclusions. B. P-T diagram for pure water (similar to LGO stage fluids) and solvi for fluids containing 5 and 10 mole percent CO_2 (MGO stage fluids). Patterned area = P-T conditions that can account for the MGO and LGO stage fluid inclusion assemblage at Carlin. Figures calculated by the methods outlined by Connolly and Bodnar (1983) and Bodnar et al. (1985). Effects of dissolved NaCl and other components are not included.

CH_4 and CO_2 clathrates on ice-melting temperature (Collins, 1979; Hanor, 1980; Hedenquist and Henley, 1985). The effects of mixed gas clathrates can also lead to uncertainties in estimated salinity (Diamond, 1994).

Apparent salinities during the HC stage ranged from a minimum of around 16.3 to >21.1 wt percent NaCl equiv. Maximum apparent salinities were also high during the BBM stage (9.7–16.7 wt % NaCl equiv, Radtke et al., 1980).

Salinity during the main gold ore stage is more difficult to constrain due to depression of $T_{m_{ice}}$ by high CO_2 contents and the effects of other gases. For example, 0.85 *m* CO_2 causes a decrease to −1.48°C (Hedenquist and Henley, 1985). Melting of metastable ice in the presence of both $CO_{2(L+V)}$ and the absence of CO_2 clathrate can account for $T_{m_{ice}}$ values as low as −4.5°C in an NaCl-free system (Burruss, 1981; Hedenquist and Henley, 1985).

Final ice-melting temperatures in group C, Dgr, and Dgp samples range from −0.2° to −6.4°C and average −2.8°C based on about 110 measurements. Final ice melting in aqueous inclusions with visible $CO_{2(L+V)}$ occurred as high as −0.3° to −0.5°C. Considering the −6.4°C value previously mentioned, maximum apparent salinity estimates for MGO stage fluids average about 5 wt percent NaCl equiv (range 1–9.5%), based on the data of Potter et al. (1978). Alternatively, clathrate-melting temperatures from group C and D quartz range from 7.3° to 9.9°C and average around 9°C for about 30 measurements. Given gas analyses suggesting about 95 percent CO_2, 5 percent CH_4, and minor H_2S (Bendrick, 1989), these clathrate-melting temperatures indicate salinities less than 5 percent and probably about 3 ± 1 wt percent NaCl equiv (Hedenquist and Henley, 1985; Collins, 1979; Diamond, 1994, fig. 18).

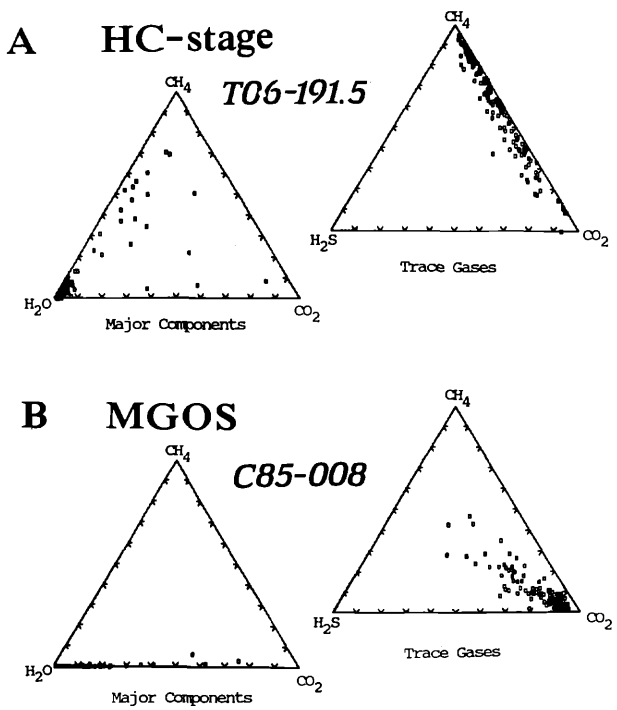

FIG. 7. Representative trace gas analyses of HC stage and MGO stage quartz samples, showing composition of bursts mainly representing single inclusions (after Bendrick, 1989). Sample C85–008 is typical mineralized MGO stage quartz (Fig. 2C); sample TO6–191.5 is quartz separated from an HC stage quartz-calcite-pyrobitumen veinlet (elev 6,089 ft, N23807, E20199).

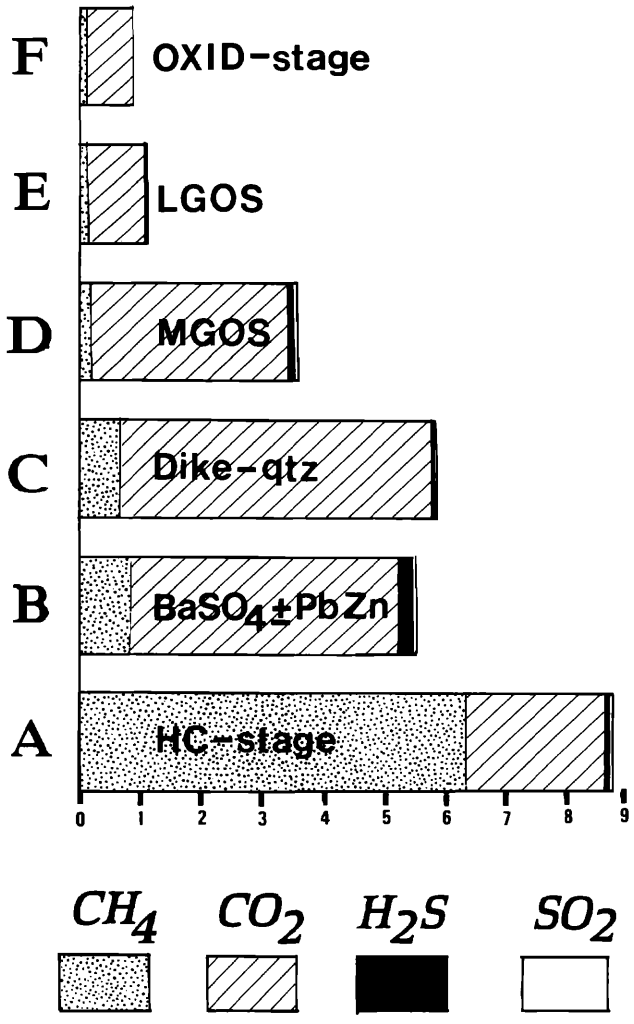

FIG. 8. Changes in gas composition as a function of paragenetic stage (after Bendrick, 1989). Horizontal axis is approximate percent of $H_2O + CH_4 + CO_2 + H_2S + SO_2$.

Because LGO stage fluids have very low salinities and could be represented by secondary inclusions in MGO stage samples, the average MGO stage salinity estimate may be biased toward a low value. Alternatively, because clathrate formation may artificially depress the final melting point of ice and could account for significant depression of the freezing point, apparent salinity estimates of the MGO stage fluids may be biased to a higher value. Acknowledging these competing effects, and considering the limited CO_2 clathrate data and its inherent caveats, the salinity of MGO stage fluids is estimated to be 3 ± 1 wt percent NaCl equiv.

Most freezing point depressions in LGO stage barite and calcite samples fall between 0° and −3.1°C and average around −0.7°C based on more than 100 measurements. Some inclusions in LGO stage samples contain a colorless solid phase which persists above 0°C, generally melts above 9.2°C, and is interpreted to be a dominantly CO_2 gas clathrate based on gas analyses of similar sample material by Bendrick (1989). These relatively high CO_2 clathrate-melting temperatures are consistent with low salinities, assuming that any other dissolved gases present have a negligible effect. Because many $T_{m_{ice}}$ values were measured at temperatures between −0.5° and 0.0°C, the maximum apparent salinities of LGO stage and later fluids are very low, even if there are small amounts of dissolved CO_2 present (Hedenquist and Henley, 1985). Maximum salinity estimates of LGO stage fluids average around 1.5 wt percent NaCl equiv and are lower than the most conservative estimates of MGO stage salinity.

Discussion of fluid inclusion studies

Several features in this study contrast with earlier fluid inclusion studies at Carlin (Nash, 1972; Radtke et al., 1980). First, the high-salinity inclusions reported by previous workers as resulting from the boiling off of salt-free vapor are probably HC stage brines trapped in early mineral phases, some of which may be enclosed by later MGO or LGO stage minerals.

Second, the reported presence of low-density H_2O-vapor inclusions which homogenized to vapor could not be confirmed. As discussed by Roedder and Bodnar (1980), Ramboz et al. (1982), Pichavant et al. (1982), and Bodnar et al. (1985), the lack of such inclusions removes the evidence for the proposed conventional boiling at Carlin.

Finally, gas-rich inclusions which represent the vapor sides of solvi in the H_2O-CH_4 (+ NaCl) and H_2O-CO_2 (+ NaCl) systems were observed in this study but are restricted to specific stages in the paragenesis. Based on H_2O-CO_2 immiscibility at Carlin, the estimated pressure during MGO stage time is at least an order of magnitude greater than the 40 bars reported by Radtke et al. (1980).

Stable Isotope Studies

Prior stable isotope data on mineral separates and whole rocks (Radtke et al., 1980; Hausen and Park, 1986; Dean et al., 1987) were used to develop the shallow-level, meteoric water hydrothermal, or boiling hot spring model for the formation of carbonate sediment-hosted disseminated gold deposits (Rye, 1985). These plus some new isotopic data (Kuehn, 1989, appendix F) are here reevaluated in light of the new paragenetic and fluid inclusion data of this study, to argue for a relatively deep geologic setting and the presence of two isotopically different fluids.

Carbon and oxygen isotopes in calcite veinlets

The $\delta^{13}C$ and $\delta^{18}O$ values of new and published data on calcite samples distinguished by stage are summarized in Figure 9.

A calcite vein of the BBM stage has a relatively high $\delta^{18}O$ value at 16.2 per mil. For a formation temperature of 225° to 250°C (Radtke et al., 1980), the calculated $\delta^{18}O_{H_2O}$ values are 8 to 9 per mil (Friedman and O'Neil, 1977) and are similar to 8 to 13 per mil for the HC stage (Kuehn, 1989). The near-zero $\delta^{13}C$ values for the HC and BBM stages appear to be largely controlled by country-rock carbonate rather than organic matter.

The majority of the $\delta^{13}C$ values for MGO and LGO stage calcite veins cluster in the range 0.0 ± 2.0 per mil (Fig. 9) and are also inferred to be determined mainly by carbon in country-rock carbonates, with little indication of lower

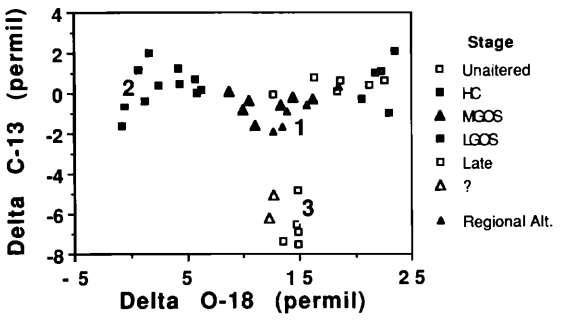

FIG. 9. Carbon and oxygen isotope values for calcite at the Carlin mine. Data from Radtke (1985) and Kuehn (1989). Path from 1 to 2 indicates most likely shift to lower $\delta^{18}O$ values during LGO stage calcite vein formation; OX stage calcite is near 3, and minor MGO stage calcite near 3 may be present (indicated by ?).

$\delta^{13}C$ values from oxidation of organic carbon. However, in many MGO and LGO stage samples, the $\delta^{18}O$ values are strongly shifted from country-rock values of 14 to 18 per mil to lower values near 0.0 per mil (Fig. 9).

Where demonstrated by crosscutting relations, later LGO stage calcite generally has lower $\delta^{18}O$ values than early LGO stage calcite. Also, some very late calcite has $\delta^{13}C$ values of −5 to −6.2 per mil, suggesting that carbon with low $\delta^{13}C$ values may have entered the system at this later time.

Oxygen isotope data on chert, jasperoid, and quartz

The $\delta^{18}O$ values of four samples of quartz selected to represent the HC, MGO, and LGO stages range from 9.6 to 27.01 per mil and span the range of published analyses of SiO_2-bearing samples from Carlin (Fig. 10).

HC stage quartz from a quartz-calcite-pyrobitumen veinlet contained the heaviest $\delta^{18}O$ value reported for Carlin samples (27‰). At 175°C the fluid in equilibrium with this quartz would have a $\delta^{18}O_{H_2O}$ value of 11.9 per mil using the calibration of Taylor (1979). These compositions correspond well with the values of 8 to 13 per mil calculated for water in equilibrium with the coexisiting HC stage calcite (Fig. 11). Several other samples, including three cherts and a cherty jasperoid, have very high $\delta^{18}O$ values (23.3–25.2‰) and may have formed under conditions similar to those of the HC stage.

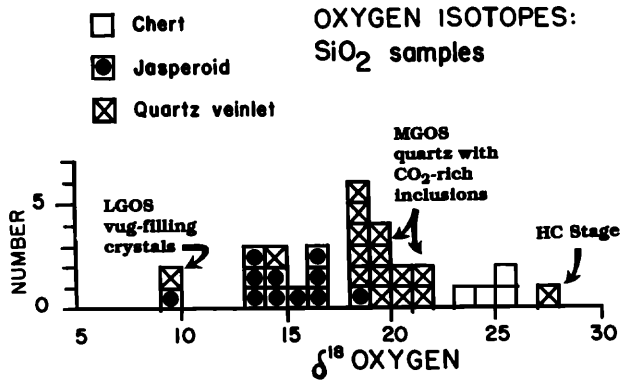

FIG. 10. Histogram of oxygen isotope values from chert, jasperoid, and quartz at the Carlin mine. Data from Kuehn (1989) and Radtke (1985). Arrows indicate the four samples analyzed in this study.

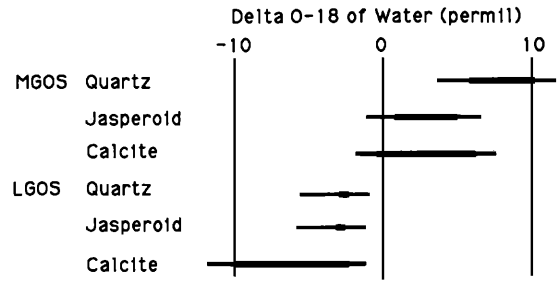

FIG. 11. Calculated oxygen isotope composition of water from which veins and jasperoids at Carlin were precipitated.

MGO stage jasperoids and quartz veinlets: MGO stage jasperoid $\delta^{18}O$ values generally lie between 13 and 17 per mil and MGO stage quartz veins have $\delta^{18}O$ values between 18 and 22 per mil (Fig. 11). For the 215° ± 30°C estimate from MGO stage quartz fluid inclusions, calculated $\delta^{18}O_{H_2O}$ values during MGO stage quartz vein formation are 4.0 to 11.5 per mil (for 185°–245°C and 18–22‰) and most probably 5 to 9 per mil for 215°C (Fig. 11). In comparison, for a similar temperature range MGO stage jasperoids indicate a fluid with $\delta^{18}O_{H_2O}$ values between −1.2 and +6.5 per mil and probably about 1 to 5 per mil. The $\delta^{18}O$ values of quartz and jasperoid thus show a wide range similar to that of the calcite samples.

CO_2-rich fluid inclusions were identified in several MGO stage (group Dgr) quartz samples with $\delta^{18}O$ values of 19.8 to 21.8 per mil. Because the gas-poor MGO stage (group Dgp) quartz sample C84-028 also has a $\delta^{18}O$ value of 21.8 per mil, the group Dgr and Dgp quartz samples probably formed from isotopically similar fluids. These high ^{18}O fluids apparently persisted locally after high CO_2 fluids.

LGO stage quartz and jasperoid: Sample C84-024B consisting of clear vug-filling microcrystals of quartz less than 1 mm long had a $\delta^{18}O$ value of 9.8 per mil. Only one East Pit jasperoid at Carlin reported by Radtke et al. (1980) had a similar low $\delta^{18}O$ value of 9.3 per mil. At temperatures of 175° to 250°C, these LGO stage samples indicate a fluid with $\delta^{18}O_{H_2O}$ values of −5.8 to −0.7 per mil (Taylor, 1979).

Isotopic data on inclusion fluids and dickite-kaolinite

One sample of HC stage quartz and two samples of group C quartz were crushed in a vacuum system and the evolved H_2O and CO_2 analyzed isotopically by Geochron Labs (Table 4A). Water in group C quartz has very low δD values of −87 and −118 per mil, suggesting meteoric origin, whereas the value from the HC stage sample is near that of seawater, as expected for diagenetic processes. The $\delta^{13}C$ values of CO_2 are slightly negative, perhaps suggesting an organic admixture to a CO_2 dominantly from carbonate.

The δD values for kaolinite-dickite from a jasperoid and a dike are very negative, as previously reported by Radtke (1985), and indicate formation from water of about −155 per mil (Table 4B).

Discussion of carbon, oxygen, and hydrogen isotope data

Barite + base metal stage: Fluids at 250° to 275°C having $\delta^{18}O_{H_2O}$ values between 8.0 and 11.0 per mil (Fried-

TABLE 4. Isotopic data (see Kuehn, 1989, for additional information)

A. Gas extractions of fluid inclusions

Sample no.	Comments	Carbon dioxide		Water	
		$\delta^{13}C_{PDB}$ (‰)	$\delta^{18}O_{SMOW}$ (‰)	δD_{SMOW} (‰)	$\delta^{18}O_{SMOW}$ (‰)
C85-005	Quartz vein in dike	−5.0	29.6	−118	−14.0
C85-017	Quartz vein in dike	−4.9	35.9	−87	−9.0
C85-030	HC stage quartz	−3.9	25.5	−9	1.7

Gas extractions and analyses by Geochron Labs

B. Dickite-kaolinite

Sample no.	Comments	δD_{SMOW} (‰)	$\delta^{18}O_{SMOW}$ (‰)	Calculated δD_{H_2O} (‰)		
				200°C	225°C	250°C
C85-023	Veins in jasperoid	−161	+2.3	−161	−153	−147
C85-025	Altered dike	−164	−0.2	−164	−156	−150
23-J	Kaolinite-sericite (Radtke, 1985)	−160		−160	−152	−146

Dickite-kaolinite is from jasperoid and an intensely altered dike in the East Pit; analyses by W. Pickthorn, U.S. Geological Survey; δD values of H_2O calculated after Friedman and O'Neill (1977)

man and O'Neil, 1977) would account for the oxygen isotope composition of barites (Radtke, 1985) as well as of the calcite sample with sphalerite (Kuehn, 1989, sample T24–66.6, table 3.6). These $\delta^{18}O_{H_2O}$ values, as well as the $\delta^{13}C$ values, are generally similar to those of the HC stage and were also dominated by the surrounding carbonate rocks.

Gold ore episode samples: The isotopic data clearly indicate at least two types of fluid during the gold ore episode. Only the calcite veinlets having the highest $\delta^{18}O$ values (near point 1 in Fig. 9) can have precipitated at <275°C from a fluid in equilibrium with MGO stage jasperoids and quartz veinlets (Fig. 11). Similarly, no samples of MGO stage quartz or jasperoid at Carlin can have precipitated in the 150° to 250°C range from a fluid with a $\delta^{18}O_{H_2O}$ value low enough to form the LGO stage calcite veins. These low $\delta^{18}O$ LGO stage calcite veins, some of which contain realgar, cinnabar, tetrahedrite, and barite, apparently precipitated from a different fluid, inferred to be unevolved meteoric water with $\delta^{18}O_{H_2O}$ values less than about −3.0 per mil.

Although a fluid with this low $\delta^{18}O_{H_2O}$ value could account for the LGO stage quartz and jasperoid samples, a fluid with a much higher $\delta^{18}O$ value is required to account for the ^{18}O values of MGO stage jasperoid and quartz veinlets. At temperatures of 200° to 225°C, minimum calculated $\delta^{18}O_{H_2O}$ values of 0.0 to 1.5 per mil are required for even the jasperoids with the lowest $\delta^{18}O$ values. Considerably higher $\delta^{18}O_{H_2O}$ values (5–9‰) are required for the MGO stage quartz veinlets, many of which cut jasperoid. These data indicate at least two separate fluids, one with relatively high $\delta^{18}O_{H_2O}$ values reflecting significant isotopic exchange with sedimentary and/or metasedimentary rocks, and one isotopically unevolved, probably reflecting relatively unexchanged meteoric water. Mixing of these two fluids is a likely explanation for most jasperoids and calcites with intermediate calculated $\delta^{18}O_{H_2O}$ values.

The alternative hypothesis—that the jasperoids formed from the same fluid as the quartz—requires temperatures in excess of 250°C, which exceeds the upper limits outlined previously. A third possibility for intermediate values is interaction with the carbonate hosts (Radtke, 1985), but the extensive dissolution of carbonate and precipitation of silica suggests that large quantities of hydrothermal water dominated the system.

According to the boiling hot spring model developed by Rye (1985), this $\delta^{18}O$ shift to lower values corresponds to oxidized zone samples and is due to influx of low-temperature ground waters. However, unoxidized MGO and LGO stage veinlet samples of this study, several containing As sulfides and sulfosalts, also show the shift to low $\delta^{18}O$ values. Thus, the strong shift to lower $\delta^{18}O$ values occurred in unoxidized rocks. In other words, the shift to lower oxygen values is not related to the process(es) responsible for oxidizing the rocks at Carlin.

The $\delta^{13}C$ values found in most of the MGO and LGO stages were apparently controlled by country-rock carbonates. This control is consistent with the large volumes of carbonate dissolved at this time. The hydrothermal fluids responsible for most calcite deposition are inferred to have changed with time from 1 to 2 in Figure 9. The lack of appreciable change in $\delta^{13}C$ values in these calcites indicates that redox reactions involving organic matter, postulated by some as an explanation for ore deposition, were minor during gold mineralization.

Two calcite samples, and CO_2 extracted from MGO stage inclusions (Table 4), have distinctly lower $\delta^{13}C$ values. These data suggest that minor amounts of carbon with lower $\delta^{13}C$ values were present during some stages of gold mineralization.

The δD values for water extracted from two samples of MGO stage quartz veins in dikes (−87 and −118‰) are significantly higher than the −140 to −153 per mil reported by Radtke et al. (1980), but the δD value of −118 per mil is similar to values from event II inclusion fluids

at Jerritt Canyon (Northrup et al., 1987; Hofstra et al., 1988).

The two dickite samples plot distinctly off the kaolinite line for weathering conditions (Taylor, 1979), having $\delta^{18}O$ values 5 to 7 per mil lower than expected for the measured δD values. This difference, as well as the identification as dickite, confirms that these clays are not supergene, but typical of hypogene clays that probably formed at temperatures above about 200° to 225°C (Field and Fifarek, 1985; Rye et al., 1992).

For the dickite samples, calculated δD_{H_2O} values for 225°C are −152 to −156 per mil (Friedman and O'Neil, 1977) and correspond well with the δD value of −153 per mil for inclusion fluids extracted from Au- and CO_2-bearing quartz samples (Q-1 and 5630-J) by Radtke et al. (1980).

If the MGO stage fluids actually have δD values less than −100 per mil, then they must be mainly meteoric. With this interpretation, the $\delta^{18}O$ values require significant oxygen isotope exchange at moderate temperatures with sedimentary or metasedimentary rocks. Alternatively, the extracted fluids might be partly from secondary inclusions containing meteoric water (Foley et al., 1982). However, the kaolinite results tend to confirm that the low δD values in fluid inclusions represent the ore stage rather than late secondary inclusions. More work is required to resolve the δD characteristics of various fluids present at Carlin and other sediment-hosted gold deposits.

Oxidation (OX) stage samples: Travertine, calcite veinlets with tan-colored oxidized halos, and calcite associated with Fe oxides have $\delta^{18}O$ values between 12.3 and 14.9 per mil, which are similar to values in both unaltered and mineralized country-rock carbonates (Fig. 9). This similarity argues for rock-dominated ^{18}O during oxidation-related processes. Assuming that late-stage meteoric waters with $\delta^{18}O_{H_2O}$ values of 0 to −10 per mil account for this oxidation of the rocks at Carlin, then temperatures of 40° to 125°C are necessary to explain these relatively high $\delta^{18}O$ values. These low temperatures are consistent with a weathering scenario for oxidation features. Oxidation stage samples also show relatively low $\delta^{13}C$ values (−4.64 to −7.55‰, Fig. 9) which is consistent with oxidation of some organic matter during this period of time.

Models of Origin

This section incorporates previous geologic, geochemical, fluid inclusion, and stable isotope data with those of the present study into a model for the formation of the Carlin gold deposit in a deep geologic setting of fluid mixing between hydrostatic and normally pressured fluids.

Depth of ore formation

A trapping pressure of 800 ± 400 bars is required by the high-density CO_2-rich fluid inclusions present in MGO stage quartz samples, given the temperatures indicated by coexisting H_2O-rich inclusions. Typical lithostatic pressure gradients of 250 bars/km require depths of at least 3.2 ± 1.6 km to reach this pressure. At a more likely gradient of 80 to 85 percent of lithostatic, which is a typical gradient for formation of vertical fractures by overpressured fluids in laterally stressed rocks (Gretener, 1981; Engelder and Lacazette, 1990), the depth would be about 3.8 ± 1.9 km. At the other extreme, passive hydrostatic load conditions involving open communication with the surface (typical of hot springs and meteoric water circulation) would require minimum formation depths of 8 ± 4 km. Depths of 6 km or more appear geologically unreasonable given the fact that HC stage veinlet orientation and fluid inclusion data define maximum depths of only about 6.1 km under conditions of lithostatic load (Kuehn, 1989), and significant burial is not documented in north-central Nevada after HC stage time (Early Cretaceous). Similarly, the 0.5- to 1.0-kbar pressures reported by Hofstra et al. (1987) at Jerritt Canyon, Nevada, for gas-rich (event IIA) fluids responsible for gold mineralization define depths of 5 to 10 km under hydrostatic conditions. Pressure gradients appreciably in excess of hydrostatic are required to account for the 1- to 5-km depths of mineralization proposed for Jerritt Canyon (Hofstra et al., 1988).

Formation of the Carlin deposit by a circulating meteoric water at 150° to 220°C under conditions approaching lithostatic seems unlikely, because a lithostatically pressured fluid could not circulate directly from the surface and because of the likely increase of the $\delta^{18}O$ value of the water during even a short residence at 3.9 ± 1.9 km and 150° to 220°C. Therefore, juxtaposition of a hydrostatic fluid with a near-lithostatic (overpressured) hydrothermal system is indicated.

Flow of the deep fluid from the overpressured to normally pressured regime would have involved throttling of the fluid, defined by abrupt pressure decrease and fluid expansion, as discussed by Barton and Toulmin (1961), Toulmin and Clark (1967), and Sims and Barton (1962). Flow is focused through the throttling zone, and active mixing of the two fluids is expected on the low-pressure side.

Under this model, the deep hot overpressured CO_2-rich fluid would ascend along fault structures to the site of the present orebody at paleodepths of 3.8 ± 1.9 km. On reaching the Roberts Mountain Formation, it would encounter an extensive zone of stratiform permeability defined by the bioclastic horizons. This zone is postulated to have contained fluid at near-hydrostatic pressure with good hydrologic connection to the surface. A pressure drop of about 500 bars is sustainable by rock strength at this depth (T. Engelder, pers. commun.). Some of the brecciation and faulting may reflect the rapid pressure transition and the accompanying rapid flow.

Fluid characteristics

Fluid inclusion and isotopic results also indicate the presence of two fluids during the gold ore episode (Table 4): (1) a gas-rich (primarily CO_2 and H_2S), moderate-salinity fluid which was ^{18}O enriched (6.5–10‰ at 225°C) as a result of considerable oxygen isotope exchange with surrounding country rocks, but is apparently dominantly of meteoric origin based on its δD values of −87 to −165 per mil, and (2) a very low salinity, relatively gas-poor fluid with both δD and $\delta^{18}O$ values typical of unevolved meteoric water. These two fluids are required to account for the wide range of $\delta^{18}O$ values in MGO and LGO stage

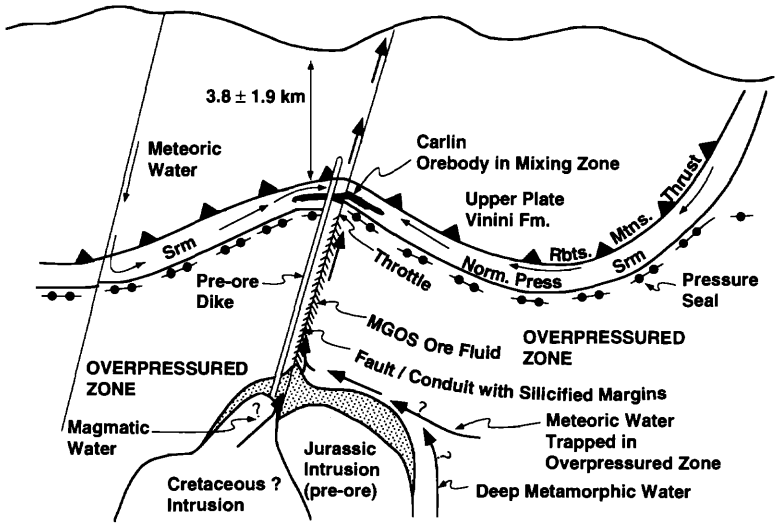

FIG. 12. Schematic diagram showing inferred environment of deposition of the Carlin ore at a throttling zone separating overpressuring from hydrostatic pressures, with resulting mixing of fluids. The deep CO_2-rich fluid may be derived from skarn formation, magmatic devolatilization, or deep metamorphism. Norm. = normal, Rbts. Mtns. = Roberts Mountains, Srm = Silurian Roberts Mountains Formation.

jasperoid and quartz and calcite veins, as well as the variable fluid inclusion characteristics of these same features.

Possible origins of the high CO_2 content of MGO stage fluids (Fig. 12) are (1) tapping of low- to moderate-grade metamorphic fluids by deep-seated structures, (2) contact metamorphism of carbonates lower in the Paleozoic section to form calc-silicates adjacent to buried intrusions, or (3) direct magmatic contribution from as yet unidentified intrusions at depth (i.e., not the Jurassic intrusive rocks exposed within about 10 km of Carlin).

An exotic source for the CO_2 is proposed because the relatively high gas contents (5–10 mole %) far exceed any contemporary geothermal analogue and require very high confining pressures not available in a near-surface meteoric water. The acquisition of CO_2 at these concentrations by ordinary water-rock interactions would require consumption of similar molalities of acid or oxidizing components (i.e., $CaCO_3 + 2H^+ = Ca^{2+} + CO_2 + H_2O$; $C_{organic} + O_2 = CO_2$). Such high molalities of acid or oxidizing species are far higher than those recorded in normal geothermal systems. Therefore, thermal breakdown of carbonates, or an igneous source, seems necessary to furnish the CO_2. The C isotope data for CO_2-rich fluid inclusions are also inconsistent with a dominantly organic origin of the CO_2 but are permissive of the other sources. Any of the above sources of CO_2 might also furnish elevated levels of H_2S by pyrite breakdown accompanying carbonate breakdown or by magmatic volatilization.

The second distinctive characteristic of MGO stage fluids is their high $\delta^{18}O_{H_2O}$ values, which require significant isotopic exchange with sedimentary rocks at high temperatures if the initial water is meteoric. Because the CO_2-rich fluids would be carbonate and silicate destructive, the original meteoric fluid was evidently heated and exchanged ^{18}O with sedimentary materials prior to acquiring the CO_2. The retention of a carbonate-destructive character despite passage through underlying carbonates before reaching the Roberts Mountain Formation seems to require flow along restricted channels bordered by silicified country rocks, as suggested by the large outcrops of jasperoid seen in surface exposures of footwall rocks.

Inclusions of LGO stage fluids in calcite and barite veins containing As ± Sb ± Hg ± Tl phases have filling temperatures of 150° to 220°C, but require an unknown pressure correction. If ore deposition occurred in a throttle between shallow hydrostatic and deeper overpressured environments at 3.8 ± 1.9 km, then for an approximate pressure correction of 10°C/km, the trapping temperature for low-temperature LGO stage inclusions might be as low as 170°C.

Possible geologic settings

The possible deep mixing environment is illustrated in Figure 12. This diagram shows a magmatic or skarn source for the CO_2 and H_2S, or an alternative source of metamorphic fluids from the middle or deep crust (Cameron, 1988). Mixing with meteoric fluids is interpreted to occur at a pressure seal separating the overpressured and normally pressured environments.

Overpressuring ("geopressuring") to values exceeding hydrostatic is reported to occur in most deep sedimentary basins (Hunt, 1990; Powley, 1990). Typically the change from overpressured to normally pressured occurs at a depth of about 3,000 m, at a seal zone with a thickness of a few hundred meters or less. The seal zone may be a relatively impermeable stratigraphic unit such as a shale or evaporite, or it may be a zone of diagenetically cemented sandstone that cuts across stratigraphic units. In addition to subhorizontal or stratigraphic boundaries, the overpressured zone may be laterally limited by steeply dipping sealed fault zones. A wide variety of causes is suggested for overpressuring, including a sedimentation rate exceeding the rate at which fluid can escape to allow compaction, tectonic compression, thermal expansion of pore

fluids, and volume increase on generation of gas or oil. Evidence from petroleum fields indicates that the seal commonly undergoes episodic leakage caused by pressures exceeding the fracture strength of the seal. During these leakage periods, oil and gas generated below the seal leak into reservoirs above the seal, presumably accompanied by water in some cases.

The formation of the Carlin deposit in a deep sedimentary basin by the involvement of two fluids with markedly different pressures, with the higher pressure fluid inferred to be overpressured relative to hydrostatic, is strongly suggestive that the deposit was formed at or just above a pressure seal. Beneath this seal lies at least 1 km of Ordovician through Lower Silurian carbonate and quartzite (Radtke, 1985), plus probably another 2 km of Cambrian rocks of similar lithology (Roberts et al., 1958). Thus, in the Carlin district, the lower Roberts Mountain Formation is the lowest unit containing significant argillaceous material in this section and may have had the low permeability necessary to form a seal. The extensive bitumen in the unit, probably in part introduced, may have served to fill porosity and decrease permeability. It is also possible that the Roberts Mountain thrust fault provided part of the seal, though somehow the meteoric LGO stage fluids reached the zone below the thrust.

Because the MGO stage fluids contain only minor CH_4 and were generated after organic material had matured past the gas window, the overpressuring during gold mineralization does not seem to have originated by methane generation or other normal sedimentary processes. The seal probably existed earlier, during the HC stage, but overpressure was regenerated in association with CO_2-rich fluids to form the ore deposits. If the seal at Carlin was stratigraphically defined by the Roberts Mountain Formation, the relative overpressuring would have been greatest along the axis of the anticline passing through the Carlin deposit, and most likely would have led to fracturing and leakage along this anticlinal zone to form the Carlin trend.

Any direct spatial, temporal, or geochemical link to intrusions that might generate CO_2-rich fluids from magmatic emanations or skarn formation is at present obscure at Carlin. Although gold ore occurs in association with skarn around Jurassic granodiorite of the Goldstrike stock, age relations and radiometric dates indicate that Carlin-type mineralization is probably 40 m.y. younger than the granodiorite and skarn (Bettles, 1989; Knutsen et al., 1991; Arehart et al., 1993c). Arehart et al. (1993c) suggest that the Welches Canyon stock, which is exposed about 10 km to the south of the Carlin district, is part of a much larger buried pluton (Mabey et al., 1978) with an age similar to that of the Carlin mineralization and may have been the origin of at least the heat for the Carlin mineralization. The high $\delta^{18}O$ of MGO stage fluids may have resulted from heating and exchange during either of the intrusive events. An alternative possibility is that the CO_2 is derived from deep crustal metamorphism and rose until sealed at approximately the Roberts Mountain Formation.

Note that the CO_2, Au, and water may have separate sources: CO_2 from magma or metamorphism, water originally meteoric, and Au from magma or leaching of sedimentary rock.

Flow of the lower pressure fluid is inferred to have been along selected permeable sedimentary horizons in the Roberts Mountain Formation, and locally, in fracture and fault zones. This unevolved meteoric water may have descended along the Roberts Mountain Formation from areas where this horizon cropped out, and along the relatively open faults expected at shallow depth.

Our model is that meteoric water trapped in sedimentary rocks prior to development of the pressure seal was set into circulation by the deeper heat source. The CO_2, H_2S, and possibly Au were added by some combination of magmatic fluids, metamorphism, and/or hydrothermal leaching. Because of the high H_2S content, Au was highly soluble in this fluid and may have been scavenged from the enclosing sediments or contributed from igneous or metamorphic sources. The development of small faults along the anticline furnished a leak (throttle) from this overpressured zone and channeled flow into permeable units in the upper Roberts Mountain Formation which were filled with cooler meteoric water. Within and beyond the throttle zone, the two fluids mixed and gold ore was precipitated. The mixed exhaust fluid then flowed upward toward the surface within the Roberts Mountain Formation and along fractures and faults.

In detail, mixing may have been facilitated by fault movements. Sibson (1987) has illustrated mineralized dilational jogs on a range of scales from millimeters to hundreds of meters in size, and has shown that these sites can be the focus of significant volumes of fluid flow. Fluid mixing will occur in dilational zones as a natural consequence of these events. In this model, gas-rich MGO stage fluids and unevolved meteoric water were drawn into lower pressure regions associated with dilational zones caused by fault movement on nonplanar structures. In addition, sudden drops in pressure could have resulted in local H_2O-CO_2 immiscibility.

Chemical effects in a fluid-mixing environment

Several chemical effects can lead to mineral deposition in the fluid-mixing environment at a throttle, including (1) dilution, (2) cooling, (3) pH changes, (4) changes in f_{O_2}, and (5) rapid local drops in pressure with the possibility of volatile exsolution. All these processes could occur nearly simultaneously, although the effects of the different factors on solubility might occur at different positions relative to the throttle. Episodic changes in flow rate and pressure conditions above the throttle would be expected to shift the precipitation locus of a given mineral with time, and to change the type of fluid present at a given site in a complex manner. The result would be a complex paragenesis and zoning, and a wide range of fluid inclusion types in individual samples, as observed at Carlin.

Northrop et al. (1987) and Hofstra et al. (1988) present compelling stable isotope evidence that mixing occurred during gold deposition at Jerritt Canyon. Hofstra et al. (1991) argue that the major gold deposition mechanism there was sulfidation of Fe oxides in the sedimentary host, in conjunction with mixing. A similar mechanism is likely at Carlin, although throttling would almost certainly

cause deposition in some form near the throttle. Throttling is not suggested at Jerritt Canyon by Hofstra et al. (1991) but is likely in view of the >500-bar pressure inferred by them in the ore fluid.

The asymmetric occurrence of gold ore, predominantly in the carbonate dissolution zone above a horizon of silicified and kaolinized permeable bioclastic feeders, but generally lacking in similarly decarbonated zones below these feeders (Kuehn and Rose, 1992), suggests that pH (carbonate interaction) was not the major control on Au solubility and that mixing in and above the permeable feeder horizons was probably crucial for depositing Au. In support of this conclusion, note that to precipitate Au, an initially acid fluid must increase in pH by several pH units, a change larger than calculations show is likely (Hayashi and Ohmoto, 1991; Hofstra et al., 1991). Oxidation also seems unlikely as a dominant precipitation mechanism, because a significantly oxidizing fluid at depth in a sequence of carbonaceous sediments is unlikely, in contrast to the proposal of Hofstra et al. (1991). The observations of Au in pyrite by Arehart et al. (1993a), the S isotope data of Arehart et al. (1993b), and the calculations of Hofstra et al. (1991) all suggest that fluid mixing and sulfidation of wall-rock Fe were the major causes of deposition.

Because silica solubility decreases markedly with temperature but is insensitive to other parameters, silicification in the feeder horizons was most likely caused by the cooling effects of mixing a hot, high Si, deep fluid with a cooler meteoric fluid in these permeable horizons.

The presence of barite in the Au ore and associated silicified zones is best explained if the deep fluid contained significant dissolved Ba but low amounts of SO_4, as is commonly found in fluids from deep sedimentary basins containing appreciable organic matter capable of reducing SO_4 to H_2S. Barite would then form by mixing this deep fluid with an SO_4-bearing meteoric fluid. A second alternative is that the deep fluid contained SO_4 in the form of HSO_4^-, since the SO_4-HSO_4 boundary is at about pH 5 at 215°C (Barnes, 1979). Neutralization of this fluid by reaction with carbonate would precipitate barite.

Conclusions

We propose that the Carlin deposit formed by the interaction of two fluids, as indicated by the major differences between the MGO and LGO stage inclusion fluids. The MGO stage fluid was CO_2 rich (5–10 mole %) with significant H_2S, a temperature of 215° ± 30°C, and a moderate salinity (3 ± 1 wt % NaCl equiv). It probably contained the dissolved Au, because a high H_2S solution at this temperature can transport considerable Au. This fluid is interpreted to have separated into CO_2-rich and CO_2-poor phases during initial stages of pressure decrease. The second (LGO stage) fluid was volatile poor with a low salinity (<0.5 wt % NaCl equiv), was cooler, and retained a meteoric $\delta^{18}O$ signature.

The high-density CO_2 inclusions representing the deep fluid require pressures of 800 ± 400 bars, indicating depths of 3.8 ± 1.9 km for a near-lithostatic gradient. This depth, in combination with recent discoveries of deep Carlin-type ores in the district, clearly shows that Carlin is not an epithermal or hot spring deposit as has been widely accepted in the past. The deep fluid that formed the Carlin deposit differs significantly from fluids observed in hot springs and shallow geothermal systems, because its high CO_2 content will not allow it to exist near the surface. Its H_2S-rich character is doubtless responsible for the high content of Au, As, Sb, Hg, and other elements that form soluble sulfide complexes. Abrupt deposition of these constituents at a zone of pressure decrease and mixing is considered to have formed the ore deposit at Carlin and probably the other Carlin-type deposits.

The common occurrence of an abrupt transition from geopressured to hydrostatically pressured in most deep sedimentary basins furnishes a favorable site for mixing with cooler meteoric waters and formation of a Carlin-type deposit by the resulting chemical changes, especially if the country rock at this location contains Fe in a form that can be sulfidized to pyrite.

The high CO_2 content in the Carlin ore fluid and the assemblage of associated elements are similar to those of the mesothermal or greenstone type of gold deposit such as the Mother Lode and Timmins districts. It is possible that the Carlin ore fluid originated in a deep metamorphic belt like these more deeply seated deposits but rose to a shallower depth before major ore deposition. However, indications of a meteoric δD signature make it more likely that some shallower process, such as skarn formation or magmatic activity within the depth range of meteoric waters, generated the fluid.

Most characteristics of the Carlin deposit are shared with other deposits of this type. High CO_2 inclusions have been observed at several such deposits (Hofstra et al., 1987; Kuehn, 1989), and a similar lithologic and structural setting in a shaly (or faulted?) zone that could be a pressure seal is widespread.

The recognition that Carlin-type deposits may form at depths of many kilometers indicates that many additional blind deposits may exist well below the present surface, in contrast to the conclusion drawn from the past inference of a shallow epithermal origin. Definition of deep structural controls, former geopressure-hydropressure transitions, and effects of spent exhaust from the volatile-rich fluid may provide guides to discovery of these deposits.

Acknowledgments

Many organizations provided valuable assistance with this research. The Carlin Gold Mining Company and its staff, especially Charles Ekburg, Odin Christensen, and Joe Rota, provided essential access, cooperation, and discussion. The U.S. Geological Survey provided field support for part of the work, and William C. Bagby and Raul J. Madrid shared freely their results on regional geology and other Carlin deposits. Robert J. Bodnar, Charles Kaiser and others at Penn State contributed to the data and interpretations on fluid inclusions and isotopes. Barbara Bakken provided valuable discussion in the field. Careful reviews by *Economic Geology* referees have contributed significantly to the final manuscript, though the authors remain responsible for any shortcomings. The major part

of the research was supported by National Science Foundation grant EAR-8407743 to A. W. Rose.

July 13, 1993; September 1, 1994

REFERENCES

Akright, R.L., Radtke, A.S., and Grimes, D.J., 1969, Minor elements as guides to gold in the Roberts Mountains Formation, Carlin gold mine, Eureka County, Nevada: Colorado School of Mines Quarterly, v. 64, p. 49–66.

Arehart, G.B., Kesler, S.E., O'Neil, J.R., and Foland, K.A., 1992, Evidence for the supergene origin of alunite in sediment-hosted micron gold deposits, Nevada: ECONOMIC GEOLOGY, v. 87, p. 263–270.

Arehart, G.B., Chryssoulis, S.L., and Kesler, S.E., 1993a, Gold and arsenic in iron sulfides from sediment-hosted disseminated gold deposits: Implications for depositional processes: ECONOMIC GEOLOGY, v. 88, p. 171–185.

Arehart, G.B., Eldridge, C.S., Chryssoulis, S.L., and Kesler, S.E., 1993b, Ion microprobe determination of sulfur isotope variations in iron sulfides from the Post/Betze sediment-hosted disseminated gold deposit, Nevada, USA: Geochimica et Cosmochimica Acta, v. 57, p 1505–1519.

Arehart, G. B., Foland, K.A., Naeser, C.W., and Kesler, S.E., 1993c, $^{40}Ar/^{39}Ar$, K/Ar and fission track geochronology of sediment-hosted disseminated gold deposits at Post-Betze, Carlin trend, northeastern Nevada: ECONOMIC GEOLOGY, v. 88, p. 622–646.

Bagby, W.C., and Berger, B.R., 1985, Geologic characteristics of sediment-hosted disseminated precious-metal deposits in the western United States: Reviews in Economic Geology, v. 2, p. 169–202.

Bakken, B.M., and Einaudi, M.T., 1986, Spatial and temporal relations between wall-rock alteration and gold mineralization, main pit, Carlin gold mine, Nevada, *in* Macdonald, A.J., ed., Gold '86: Willowdale, Ontario, Konsult International, p. 388–403.

Barker, C., and Smith, M.P., 1986, Mass spectrometric determination of gases in individual fluid inclusions in natural minerals: Analytical Chemistry, v. 58, p. 1330–1333.

Barnes, H.L., 1979, Solubilities of ore minerals, *in* Barnes, H.L., Geochemistry of hydrothermal ore deposits: New York, Wiley Interscience, p. 409.

Barton, P.B., and Toulmin, P., 1961, Some mechanisms for cooling hydrothermal fluids: U.S. Geological Survey Professional Paper 424B, p. 348–352.

Bendrick, M.B., 1989, Mass spectrometric analysis of gases in fluid inclusions from the Carlin gold deposit, Eureka County, Nevada: Unpublished M.S. thesis, Tulsa, OK, University of Tulsa, 205 p.

Berger, B.R., 1985, Geological and geochemical relationships at the Getchell mine and vicinity, Humboldt County, Nevada: Discoveries of epithermal precious metal deposits, *in* Case histories of mineral discoveries, v. 1: New York, Society of Mining Engineers, p. 51–59.

Bettles, K.H., 1989, Gold deposits of the Goldstrike mine, Carlin trend, Nevada: Society of Mining Engineers Preprint 89–158, 14 p.

Bodnar, R.J., Reynolds, T.J., and Kuehn, C.A., 1985, Fluid inclusion systematics in epithermal systems: Reviews in Economic Geology, v. 2, p. 73–98.

Burruss, R.C., 1981, Analysis of phase equilibria in C-O-H-S fluid inclusions, *in* Short course in fluid inclusions—applications to petrology: Calgary, Mineralogical Association of Canada, p. 39–74.

Burton, J.C., Lawler, J.P., and Ayres, D.E., 1985, Genesis of Carlin-type gold deposits [abs.]: Geological Society of America Abstracts with Programs, v. 17, p. 536.

Cameron, E.M., 1988, Archean gold: Relation to granulite formation and redox zoning in the crust: Geology, v. 16, p. 109–112.

Collins, P.L.F., 1979, Gas hydrates in CO_2-bearing fluid inclusions and the use of freezing data for salinity: ECONOMIC GEOLOGY, v. 74, p. 1435–1444.

Connolly, J.A.D., and Bodnar, R.J., 1983, A modified Redlich-Kwong equation of state for H_2O-CO_2 mixtures: Applications to fluid inclusion studies [abs.]: EOS, v. 64, p. 350.

Dean, W.E., Pratt, L.M., Brigg, P.H., Daws, T.A., Engleman, E.E., Jackson, L., Layman, L.R., Ryder, J.L., Stone, C.L., Threlkeld, C.N., and Vuletich, A.K., 1987, Data on the geochemistry of Carlin-type disseminated gold deposits and associated rocks, north-central Nevada: U.S. Geological Survey Open-File Report 87–446, 19 p.

Diamond, L.W., 1994, Salinity of multivolatile fluid inclusions determined from clathrate hydrate stability: Geochimica et Cosmochimica Acta, v. 58, p. 19–41.

Dickson, F.W., Radtke, A.S., and Peterson, J.A., 1979, Ellisite, Tl_3AsS_3, a new mineral from the Carlin gold deposit, Nevada, and associated sulfide and sulfosalt minerals: American Mineralogist, v. 64, p. 701–707.

Engelder, T., and Lacazette, A., 1990, Natural hydraulic fracturing, *in* Barton, N., and Stephansson, O., eds., Rock joints: Rotterdam, A.A. Balkema, p. 35–43.

Evans, J.G., and Peterson, J.A., 1986, Distribution of minor elements in the Rodeo Creek NE and Welches Canyon quadrangles, Eureka County, Nevada: U.S. Geological Survey Bulletin 1657, 65 p.

Field, C.W., and Fifarek, R.H., 1985, Light stable isotope systematics in the epithermal environment: Reviews in Economic Geology, v. 2, p. 99–128.

Foley, N.K., Bethke, P.M., and Rye, R.O., 1982, A re-interpretation of delta D_{H_2O} values of inclusion fluids in quartz from shallow orebodies [abs.]: Geological Society of America Abstracts with Programs, v. 15, p. 489–490.

Friedman, I., and O'Neil, J.R., 1977, Compilation of stable isotope fractionation factors of geochemical interest: U.S. Geological Survey Professional Paper 440-KK, 12 p.

Gehrig, M., 1980, Phasengleichgewichte und PVT-Daten ternarer Mischingungen aus Wasser, Kohlendioxide und Natriumchloride: Unpublished Ph.D. thesis, Karlsruhe, Germany, Institute fur Physikallische Chemie, Universitate Karlsruhe, 148 p. (in German).

Gretener, P.E., 1981, Pore pressure: Fundumentals, general ramifications and implications for structural geology: American Association of Petroleum Geologists, Education Course Note Series, no. 4, 131 p.

Hall, H. T., and Yund, R.A., 1964, Equilibrium relations among some silver sulfosalts and arsenic sulfides [abs.]: Americal Geophysical Union Transactions, v. 45, p. 122.

Hanor, J.S., 1980, Dissolved methane in sedimentary brines: Potential effect on the PVT properties of fluid inclusions: ECONOMIC GEOLOGY, v. 75, p. 603–609.

Hardie, B.S., 1966, Carlin gold mine, Lynne district, Nevada: Nevada Bureau of Mines Report 13, part A, p. 73–83.

Hausen, D.M., 1967, Fine gold occurrence at Carlin, Nevada: Unpublished Ph.D. dissertation, New York, Columbia University, 166 p.

Hausen, D.M. and Kerr, P.F., 1968, Fine gold occurrence at Carlin, Nevada, *in* Ridge, J.D., ed., Ore deposits of the United States, 1933–1967 (Graton-Sales vol.): New York, American Institute of Mining, Metallurgical and Petroleum Engineers, p. 908–940.

Hausen, D.M., and Park, W.C., 1986, Observations on the association of gold mineralization with organic matter in Carlin-type ores, *in* Organics and ore deposits: Denver Region Exploration Geologists Society, Proceedings, v. 2, p. 119–136.

Hayashi, K.I., and Ohmoto, H., 1991, Solubility of gold in NaCl- and H_2S-bearing aqueous solutions at 250–350°C: Geochimica et Cosmochimica Acta, v. 55, p. 2111–2126.

Hedenquist, J.W. and Henley, R.W., 1985, The importance of CO_2 on freezing-point measurements of fluid inclusions: Evidence from active geothermal systems and implications for epithermal ore deposition: ECONOMIC GEOLOGY, v. 80, p. 1379–1406.

Hofstra, A.H., Landis, G.P., and Rowe, W.A., 1987, Sediment-hosted disseminated gold mineralization at Jerritt Canyon, Nevada. IV—Fluid geochemistry [abs.]: Geological Society of America Abstracts with Programs, v. 19, p. 704.

Hofstra, A.H., Northrup, H.R., Rye, R.O., Landis, G.P., and Birak, D.J., 1988, Origin of sediment-hosted gold deposits by fluid mixing—evidence from jasperoids in the Jerritt Canyon gold district [abs.]: Bicentennial Gold '88, Melbourne, Australia, May, 1988, Extended Oral Abstracts, p. 284–289.

Hofstra, A.H., Leventhal, J.S., Northrop, H.R., Landis, G.P., Rye, R.O., Birak, D.J., and Dahl, A.R., 1991, Genesis of sediment-hosted disseminated-gold deposits by fluid mixing and sulfidization: Chemical-reaction-path modeling of ore-depositional processes documented in the Jerritt Canyon district, Nevada: Geology, v. 19, p. 36–40.

Hunt, J.M., 1990, Generation and migration of petroleum from abnormally pressured fluid compartments: American Association Petroleum Geologists Bulletin, v. 74, p. 1–12.

Ilchick, R.P., 1995, $^{40}Ar/^{39}Ar$, K/Ar and fission track geochronology of the sediment-hosted disseminated gold deposits at Post-Betze, Carlin

trend, northeastern Nevada—a discussion: ECONOMIC GEOLOGY, v. 90, p. 208–210.

Joralemon, P., 1951, The occurrence of gold at the Getchell mine, Nevada: ECONOMIC GEOLOGY, v. 46, p. 267–310.

—— 1975, K-Ar relations of granodiorite emplacement and tungsten and gold mineralization near the Getchell mine, Humboldt County, Nevada—a discussion: ECONOMIC GEOLOGY, v. 70, p. 405–406.

Knutsen, G.C., Zimmerman, C.J., and Christensen, O.D., 1991, Current geologic research and deep deposits of the Carlin trend, northeast Nevada: The Gangue (Geologic Association of Canada, Mineral Deposits Division), no. 34, p. 3–5.

Kuehn, C.A., 1989, Studies of disseminated gold deposits near Carlin, Nevada: Evidence for a deep geologic setting of ore formation: Unpublished Ph.D. thesis, University Park, PA, Pennsylvania State University, 396 p.

Kuehn, C.A., and Rose, A.W., 1986, Temporal framework for the development of fluids at the Carlin gold mine, Eureka County, Nevada [abs.]: Geological Society of America Abstracts with Programs, v. 18, p. 663.

—— 1992, Geology and geochemistry of wall-rock alteration at the Carlin gold deposit, Nevada: ECONOMIC GEOLOGY, v. 87, p. 1697–1721.

Mabey, D.R., Zeitz, I., Eaton, G.P., and Kleinkopf, M.D., 1978, Regional magnetic patterns in part of the Cordillera in the western United States: Geological Society of America Memoir 152, p. 93–106.

Madrid, R.J., and Bagby, W.C., 1986, Vein paragenesis in selected sediment-hosted gold deposits in north-central Nevada [abs.]: Geological Society of America Abstracts with Programs, v. 18, p. 393.

—— 1988, Gold occurrence and its relation to vein and mineral paragenesis in selected sedimentary-rock-hosted, Carlin-type deposits in Nevada [abs.]: Bicentennial Gold '88, Melbourne, Australia, May 1988, Extended Abstracts Volume, p. 161–166.

McDougall, I., and Harrison, T.M., 1988, Geochronology and thermochronology by the $^{40}Ar/^{39}Ar$ method: New York, Oxford University Press, 120 p.

Nash, J.T., 1972, Fluid-inclusion studies of some gold deposits in Nevada: U.S. Geological Professional Paper 800-C, p. C15–C19.

Northrop, H.R., Rye, R.O., Landis, G.P., Lustwerk, R., Jones, M.B., and Daly, W.E., 1987, Sediment-hosted disseminated gold mineralization at Jerritt Canyon. V—Stable isotope geochemistry and a model of ore deposition [abs.]: Geological Society of America Abstracts with Programs, v. 19, p. 791.

Osterberg, M.K., 1989, The geology and geochemistry of the Chimney Creek gold deposit, Osgood Mountains, Churchill County, Nevada: Unpublished Ph.D. thesis, Tucson, University of Arizona, 255 p.

Parratt, R.L., and Bloomstein, E.I., 1989, Discovery, geology, and mineralization of the Rabbitt Creek gold deposit, Humboldt County, Nevada [abs.]: Society of Mining Engineers, Annual Meeting, Las Vegas, NV, February 1989, Abstracts with Program, p. 108.

Pasteris, J.D., Kuehn, C.A., and Bodnar, R.J., 1986, Applications of the laser Raman microprobe RAMANOR U-1000 to hydrothermal ore deposits: Carlin as an example: ECONOMIC GEOLOGY, v. 82, p. 915–930.

Pichavant, M., Ramboz, C., and Weisbrod, A., 1982, Fluid immiscibility in natural processes: Use and misuse of fluid inclusion data. I. Phase equilibria analyses—a theoretical and geometrical approach: Chemical Geology, v. 37, p. 1–37.

Potter, R.W., II, Clynne, M.A., and Browne, D.L., 1978, Freezing point depression of aqueous sodium chloride solutions: ECONOMIC GEOLOGY, v. 73, p. 284–285.

Powley, D.E., 1990, Pressures and hydrogeology in petroleum basins: Earth Science Reviews, v. 29, p 215–226.

Radtke, A.S., 1985, Geology of the Carlin gold deposit, Nevada: U.S. Geological Survey Professional Paper 1267, 124 p.

Radtke, A.S., Rye, R.O., and Dickson, F.W., 1980, Geology and stable isotope studies of the Carlin gold deposit, Nevada: ECONOMIC GEOLOGY, v. 75, p. 641–672.

Ramboz, C., Pichavant, M., and Weisbrod, A., 1982, Fluid immiscibility in natural processes: Use and misuse of fluid inclusion data. II. Interpretation of fluid inclusion data in terms of immiscibility: Chemical Geology, v. 37, p. 29–48.

Roberts, R.J., 1986, The Carlin story: Nevada Bureau of Mines and Geology Report 40, p. 71–80.

Roberts, R.J., Hotz, P.E., Gilluly, J., and Ferguson, H.G., 1958, Paleozoic rocks of north-central Nevada: American Association of Petroleum Geologists Bulletin, v. 42, p. 2813–2857.

Roberts, R.J., Radtke, A.S., Coats, R.R., Silberman, M.L., and McKee, E.H., 1971, Gold-bearing deposits in north-central Nevada and southwestern Idaho; with a section on periods of plutonism in north-central Nevada: ECONOMIC GEOLOGY, v. 66, p. 14–33.

Roedder, E., 1984, Fluid inclusions: Reviews in Mineralogy, v. 12, 644 p.

Roedder, E., and Bodnar, R.J., 1980, Geologic pressure determinations from fluid inclusion studies: Annual Review of Earth and Planetary Sciences, v. 8, p. 263–301.

Rota, J.C., 1987, Geology of Newmont Gold Company's gold quarry deposit, Eureka County, Nevada, *in* GeoExpo '86, Exploration in the North American Cordillera: Vancouver, Association of Exploration Geochemists, p. 42–50.

Rye, R.O., 1985, A model for the formation of carbonate-hosted disseminated gold deposits based on geologic, fluid-inclusion, geochemical, and stable-isotope studies of the Carlin and Cortez deposits, Nevada: U.S. Geological Survey Bulletin 1646, p. 95–105.

Rye, R.O., Bethke, P.M., and Wasserman, M.D., 1992, The stable isotope geochemistry of acid sulfate alteration: ECONOMIC GEOLOGY, v. 87, p. 225–262.

Seedorff, E., 1991, Magmatism, extension and ore deposits of Eocene to Holocene age in the Great Basin—mutual effects and preliminary proposed genetic relationships, *in* Raines, G.L., Lisle, R.E., Schafer, R.W., and Wilkinson, W.H., eds., Geology and ore deposits of the Great Basin: Reno, Geolgoical Society of Nevada, p. 133–178.

Sibson, R.H., 1987, Earthquake rupturing as a mineralizing agent in hydrothermal systems: Geology, v. 15, p. 701–704.

Sims, P.K., and Barton, P.B., 1962, Hypogene zoning and ore genesis, Central City district, Colorado, *in* Petrologic studies, a volume to honor A.F. Buddington: Boulder, CO, Geological Society of America, p. 373–395.

Sterner, S.M., and Bodnar, R.J., 1989, Synthetic fluid inclusions. VII. Re-equilibration of fluid inclusions in quartz during laboratory-simulated metamorphic burial and uplift: Journal of Metamorphic Petrology, v. 7, p. 243–260.

Taylor, H.P., Jr., 1979, Oxygen and Hydrogen isotope relationships in hydrothermal mineral deposits, *in* Barnes, H.L., ed., Geochemistry of hydrothermal ore deposits: New York, Wiley, p. 236–273.

Tissot, B.P., and Welte, D.H., 1984, Petroleum formation and occurrence, 2nd ed.: New York, Springer-Verlag, 699 p.

Toulmin, P., and Clark, S.P., 1967, Thermal aspects of ore formation, *in* Barnes, H.L., ed., Geochemistry of hydrothermal ore deposits: New York, Holt, Rhinehart, and Winston, p. 437–464.

Weissberg, B.G., Browne, P.R.L., and Seward, T.M., 1979, Ore metals in active geothermal systems, *in* Barnes, H.L., ed., Geochemistry of hydrothermal ore deposits: New York, Wiley Interscience, p. 738–780.